LJMU Research Online

Milano, S, Lindauer, S, Prendergast, AL, Hill, EA, Hunt, CO, Barker, G and Schöne, B

 Mollusk carbonate thermal behavior and its implications in understanding prehistoric fire events in shell middens

http://researchonline.ljmu.ac.uk/id/eprint/8826/

Article

For more information please contact researchonline@ljmu.ac.uk

Mollusk carbonate thermal behaviour and its implications in understanding prehistoric fire events in shell middens

Stefania Milano[1,2*], Susanne Lindauer[3], Amy L. Prendergast[4], Evan A. Hill[5], Chris O. Hunt[6], Graeme Barker[7], Bernd R. Schöne[2]

[1] Department of Human Evolution, Max Planck Institute for Evolutionary Anthropology, Deutscher Platz 6, 04103 Leipzig, Germany
[2] Institute of Geosciences, University of Mainz, Joh.-J.-Becherweg 21, 55128 Mainz, Germany
[3] Curt-Engelhorn-Zentrum Archaeometry gGmbH, Klaus-Tschira-Archaeometry-Centre, C4, 8, 68159 Mannheim, Germany.
[4] School of Geography, University of Melbourne, 221 Bouverie St, Carlton, 3053, VIC, Australia
[5] School of Natural and Built Environment, Queens University Belfast, Elmwood Ave, Belfast BT9 6AY, UK
[6] School of Natural Sciences and Psychology, Liverpool John Moores University, Byrom Street, Liverpool, United Kingdom
[7] McDonald Institute for Archaeological Research, University of Cambridge, Downing St, Cambridge CB2 3ER, UK

* Corresponding author. Email: stefania_milano@eva.mpg.de

Abstract

Archaeological shell middens are particularly important for reconstructing prehistoric human subsistence strategies. However, very little is known about shellfish processing, especially when related

32 to the use of fire for dietary and disposal purposes. To shed light on prehistoric food processing

33 techniques, an experimental study was undertaken on modern gastropod shells (*Phorcus lineatus*). The

34 shells were exposed to high temperatures (200-700 °C) to investigate subsequent mineralogy and macro-

35 and microstructural changes. Afterwards, the three-pronged approach was applied to archaeological

36 shells from Haua Fteah cave, Libya (*Phorcus turbinatus*) and from shell midden sites in the United Arab

37 Emirates (*Anadara uropigimelana* and *Terebralia palustris*) to determine exposure temperatures.

38 Results indicated that shells from the Haua Fteah were exposed to high temperatures (600 - 700 °C)

39 during the Mesolithic period (c. 12.7 - 9 ka), whereas specimens from the Neolithic period (c. 8.5 - 5.4

40 ka) were mainly exposed to lower temperatures (300 - 500 °C). The thermally-induced changes in *A.*

41 *uropigimelana* and *T. palustris* shells from the South East Arabian archaeological sites were similar to

42 those seen in *Phorcus* spp. suggesting a broad applicability of the experimental results at an interspecific

43 level. Although heat significantly altered the appearance and mineralogy of the shells, $^{14}C_{AMS}$ ages

44 obtained on burnt shells fit within the expected age ranges for their associated archaeological contexts,

45 indicating that robust radiocarbon ages may still be obtained from burnt shells. Our study indicates that

46 the combination of microstructural and mineralogical observations can provide important information to

47 infer shellfish processing strategies in prehistoric cultures and their change through time.

48

49

50

1. Introduction

52 Shells grow incrementally throughout the lifetime of mollusks and function as protection and support

53 structures. Shells also serve as excellent palaeoenvironmental archives (i.e. Jones, 1983; Schöne et al.,

2004; Butler et al., 2013), because they faithfully record the physical and chemical conditions of their ambient environment and temporal changes to these. Such information is stored in the form of geochemical and structural properties (Epstein, 1953; Goodwin et al., 2001; Schöne, 2008). Sclerochronology is the research field that studies the temporal context of shell chemical composition (i.e. stable isotopes and trace elements) and physical accretionary patterns to produce extremely highly resolved palaeoenvironmental reconstructions (Schöne et al., 2005; Miyaji et al., 2007; Milano et al., 2017; Oschmann, 2009). For example, shell oxygen isotope content ($\delta^{18}O_{shell}$) is routinely used as paleothermometer (Schöne et al., 2005; Ferguson et al., 2011; Prendergast et al., 2013; Prendergast and Schöne, 2017).

A rapidly growing interest in the research field of sclerochronology supports the spread of its methodologies and approaches to different disciplines such as archaeology and environmental biomonitoring (Mannino and Thomas, 2002; Andrus, 2011; Steinhardt et al., 2016; Schöne and Krause, 2016). The analysis of mollusk shell material is especially relevant within the framework of prehistoric archaeology. Shellfish have been an important dietary component since the emergence of anatomically modern humans (~ 300 kyr ago; de Lumley, 1966), due to their easy accessibility, reliable availability throughout the year and source of proteins and micronutrients essential for physical development (Erlandson, 2001; Broadhurst et al., 2002; Marean et al., 2007; Fa, 2008).

The application of sclerochronology substantially broadens the potential use of mollusk shells in archaeology. Besides being suitable palaeoenvironmental archives, the shells become a key tool for understanding the response of human behaviour to climatic changes. For instance, $\delta^{18}O_{shell}$ is used to constrain the season of mollusk collection (Mannino et al., 2007; Burchell et al., 2013; Prendergast et

al., 2016). In turn, seasonality provides information on the seasonal mobility of hunter-gatherer societies and helps to identify whether sites were permanently or ephemerally occupied (Shackleton, 1973; Mannino and Thomas, 2002; Eerkens et al., 2013). However, the processes related to mollusk preparation, consumption and disposal are still largely unknown (Milano et al., 2016). In some cases, it has been observed a modification of the shell structure by removal of the gastropod apex with stone tool, thorn or canine tip to allow the mollusk to be sucked out (Girod, 2011). As for bivalves, the shells were sometimes scarred or wholesale smashed (Hammond, 2014). Evidence of pyrotechnology associated with mollusk shell middens suggests that a certain degree of heat exposure may have been involved in some cases (Erlandson et al., 1999; Berna and Goldberg, 2008; Taylor et al., 2011). However, few studies have addressed the reconstruction of such processes in the framework of prehistoric marine resource exploitation (Andrus and Crowe, 2002; Aldeias et al., 2016; Milano et al., 2016) and this study will be the first instance where this has been carried out.

The present study builds upon previous work by Milano et al. (2016) who found that significant structural and chemical changes occurred in modern mollusk shells when they were heated at ≥ 300 °C for 20 minutes or more. Here, we investigate the effects of a shorter heat exposure (5 minutes), since shellfish are generally thought to be processed for short periods of time. To achieve this aim, modern *Phorcus lineatus* are used as a calibration tool to understand the response to thermal treatments at the macro-, microstructural and geochemical level. These findings are then applied to archaeological specimens from the Haua Fteah, eastern Libya (*Phorcus turbinatus*) to test whether high temperatures exposure can be detected in archaeological shells of the same genus using the three-pronged approach developed in the experimental phase. Archaeological specimens from the United Arab Emirates (*Anadara uropigimelana* and *Terebralia palustris*) are used to understand the efficacy of this three-

pronged approach on a broader scale to other mollusk species. Furthermore, given the importance of

shells for radiocarbon dating coastal sites and the abundance of burnt shells in middens (Douka et al.,

2014; Lindauer et al., 2016), we present preliminary results on the influence of thermal alterations on

shell radiocarbon dating results.

2. Materials and methods

A total of 41 shells were analysed (Table 1). Fifteen live-collected shells of *P. lineatus* were used for the

experimental phase. The archaeological material consisted of eighteen specimens of *P. turbinatus*

selected from key occupation contexts in the Mesolithic and Neolithic layers from the Haua Fteah cave

in Libya, as well as six specimens of *A. uropigimelana* and two specimens of *T. palustris* from shell

midden sites near Kalba in the United Arab Emirates (Fig. 1).

2.1 Shell material: *P. lineatus* and *P. turbinatus*

Phorcus spp. are rocky shore gastropods living in the intertidal zone along the Mediterranean (*P.*

turbinatus: Menzies et al., 1992; Schembri et al., 2005; Mannino et al. 2008; Prendergast et al., 2013)

and Eastern North Atlantic coasts (*P. lineatus:* Kendall, 1987; Donald et al., 2012; Gutiérrez-Zugasti et

al., 2015). Both species are sensitive to seasonal environmental changes, specifically water temperature

fluctuations. Furthermore, they are extremely abundant in prehistoric sites of this region (Mannino and

Thomas, 2001; Colonese et al., 2011; Hunt et al. 2011; Bosch et al., 2015; Gutiérrez-Zugasti et al.,

2015). Therefore, many previous studies have used their geochemical data for palaeoenvironmental

reconstructions (Mannino et al., 2003; Colonese et al., 2009; Prendergast et al., 2016).

122   In the present study, *P. lineatus* (previously known as *Osilinus lineatus* and *Monodonta lineata*)

123   was selected as a modern reference and *P. turbinatus* (previously known as *Osilinus turbinatus*,

124   *Monodonta turbinata* and *Trochocochlea turbinata*) for the archaeological case study. Despite being

125   two distinct species, they share similar shell shape, size and the same microstructural organization and

126   mineralogy and they live within the same microenvironments on the Mediterranean and Atlantic coasts.

127   Their shell consists of two aragonitic layers with specific organizations. The outer shell layer (oSL) is

128   arranged in spherulitic prismatic microstructures whereas the inner shell layer (iSL) consists of nacre

129   (Mannino et al., 2008; Milano et al., 2016). The minor phenotypic and taxonomically relevant

130   differences between the two species in shell coloration and aperture size likely do not influence the

131   structural behaviour of the shell in reaction to thermal stress.

132

133

134   2.2 Shell material: *A. uropigimelana* and *T. palustris*

135   *A. uropigimelana* and *T. palustris* inhabit tropical mudflats. *A. uropigimelana* is a bivalve of the Arcidae

136   family (ark clams), which is widely distributed in East Africa and the Central Pacific. It lives in shallow

137   waters (1-8 m) in association with seagrass beds and can reach 45 years of age (Tebano and Paulay,

138   2001; Petchey et al., 2013). *T. palustris,* also known as mud whelk, is one of the largest gastropods of

139   mangrove-dominated habitats in the Pacific Ocean (Plaziat, 1984; Houbrick, 1991; Carlen and Olafsson,

140   2002). It is typically found in the intertidal zone and its lifespan is currently unknown. Possibly the adult

141   size is reached after about four years, when it moves from offshore environments into the mangrove

142   settings (Nishihira et al., 2002). Both species are very abundant in the prehistoric record in the Arabian

143   Sea region (Biagi et al., 1984; Beech and Kallweit, 2001; Gardner, 2005; Lindauer et al., 2017).

144

145   The shell of *A. uropigimelana* is entirely aragonitic and consists of three layers. The oSL is

146   organized in branching crossed-lamellar structures, the middle shell layer (mSL) is formed of linear-

147   crossed lamellae and the iSL is characterized by irregular complex-crossed lamellae. Likewise, the shell

148   of *T. palustris* is aragonite and is organized in simple-crossed lamellar (oSL and iSL) and linear-crossed

149   lamellar microstructures (mSL). The terminology follows the author´s observations and the description

150   from Carter et al. (2012).

151

152

153   2.3 Modern and archaeological settings

154   Modern specimens of *P.lineatus* were collected from Praia do Tamariz, Portugal (38.7036 °N, -9.4038

155   °E) on 10 August 2016. The shells were gathered from a rocky portion in the mid-intertidal zone just

156   outside the estuary of the Tajo River on the Atlantic coast (Fig. 1). To minimize the effects of ontogeny

157   on the stable isotope results, shells with similar sizes were selected. Maximum shell height ranged

158   between 12 and 14.3 mm and the maximum shell width ranged between 13.3. and 15.7 mm. This size

159   class represents the average shell size of *P.lineatus* adult population in the region (da Costa, 2015).

160   Immediately after collection, the specimens were frozen for about one hour and subsequently the soft

161   tissues were removed.

162

163   The archaeological remains of *P. turbinatus* were collected from the Haua Fteah cave, Libya (Fig.

164   1). The Haua Fteah cave was first excavated in 1951-1955 by Charles McBurney, who cut a 14 m-deep

165   stepped trench from the level of the present cave floor, exposing a deep sequence of occupation dating

166   from the last intergacial to the Holocene (McBurney, 1967). New excavations (ERC:TRANSNAP)

167   coordinated by Prof. Graeme Barker between 2008-2015 reopened the McBurney trench and cut an

168   overlapping series of small trenches down its southern face (Barker et al., 2010, 2012; Farr et al., 2013).

169   Eleven of the eighteen specimens used in this study were from Trench U, a small (0.75 m x 1 m) cutting

170   in the upper 2 m of the sediments which exposed occupation levels of Neolithic character and age. The

171   Neolithic phase in the cave has a modelled age of ca. 8.5 - 5.4 cal. BP (Douka et al., 2014). These shells

172   were excavated in 2012 from contexts 742, 743 and 747. These sediments, especially context 747, were

173   associated with evidence of extensive burning in form of frequent charcoal, visibly charred animal bone

174   and shell, and lithic artefacts with thermoclastic fractures. Seven specimens were selected from Trench

175   M, a 2 m x 1 m trench cut down the same side of the McBurney trench at ca. 2-8 m depth. The

176   specimens were excavated in 2009 and 2010 from contexts 10,002, 10,005 and 10,006, which have been

177   dated to the Early Holocene and can be ascribed to the Mesolithic Capsian phase of occupation defined

178   by McBurney (1967). The sediments were similar in character to those of Trench U in terms of their

179   plentiful evidence for firing events.

180

181   The archaeological remains of *A. uropigimelana* and *T. palustris* were excavated from open sites

182   on the Gulf of Oman coast in the United Arab Emirates (Fig. 1). Specimen KS Ana1, KSM UBL Ana2,

183   KK1 Ana3 and KK1 Ana4 came from the shell midden KK1 situated near the mangroves at Kalba,

184   along the northern coast of the Gulf of Oman (Lindauer et al., 2016). Specimen KS Ana1 was found on

185   the beach nearby and it yielded a radiocarbon age of 7328-7113 cal. BP. It may have remained in the

186   mangrove sediments or in the sabkha (salt flat) since Neolithic times or perhaps washed out recently

187   from an archaeological midden where it was found on the beach. This would also explain its good

188   preservation. The shell midden KK1 is at the outermost edge of the sabkha of the mangrove at Kalba

189   and contains only material from the Neolithic, in two distinct phases. These are reflected in the shell [14]C

190   ages that range from ca. 7146 - 6946 cal. BP at the base to ca. 6600 - 6450 cal. BP at the surface (1σ).

191

192   Specimens K4 SL Ana3, K4 SL GA1, K4 BZ GT1 and K4 BZ UGT1 were excavated from site

193   Kalba K4, lying close to the modern town of Kalba north of a mangrove area. This site has evidence of

194   settlement structures that can be ascribed to the Bronze Age and Iron Age. Two distinct layers (MBZ 1

195   and MBZ 2) situated close to an Iron Age mudbrick wall contain a large amount of shells, both burnt

196   and unburnt, together with charcoal fragments. The lower layer (MBZ1) contained fewer shells than the

197   immediately overlying layer MBZ2. Both layers are around 30 cm thick. Dating measurements show

198   that both layers can be ascribed to the Middle Bronze Age (Lindauer et al., 2017). The shells of the

199   lower MBZ1 have a mean age of ca. 3882 - 3727 cal. BP and the upper MBZ2 shells of ca. 3695 - 3641

200   cal. BP. The results are in accordance with the archaeological data from previous excavations (Phillips

201   and Mosseri-Marlio, 2002).

202

203

204   2.4 Experimental design

205   The experiment on modern shells followed a similar protocol to that described by Milano et al. (2016).

206   However, in this case the shells were exposed to different temperatures for 5 min. The choice of this

207   duration was twofold: (1) to identify potential changes in shell behaviour after short (5 min) heat

208   exposure as compared with the medium (20 min) and long (60 min) heat exposures that were tested in

209   the previous study (Milano et al. 2016) and (2) to attempt to reconstruct the temperatures at which

210   archaeological shellfish were processed. Sparse ethnographic observations (e.g. Meehan, 1977, 1982) as

211   well as modern traditions (e.g. Smith, 1978) suggest that the bivalves are processed for only few minutes

212   before consumption.

213

214   The shells were heated at 200 °C, 300 °C, 400 °C, 500 °C, 600 °C and 700 °C in a high

215   temperature tube furnace. Specimens were placed in the furnace when the desired temperature was

216   stabilized to ensure the reproducibility of the experiment and to minimize the noise deriving by

217   temperature fluctuations. In order to record potential weight loss, each shell was weighted before and

218   after the roasting experiment to the nearest 1 mg.

219

220

221   ## 2.5 Shell preparation

222   To study the specimens, modern and archaeological shells were fully embedded in Struers EpoFix resin

223   and air-dried for 24 hours. This strategy prevented the shells from breaking during the following

224   preparation steps. Each resin block was glued to a plexiglass cube and a low-speed precision saw

225   (Buehler Isomet 1000) was used to cut two sections (ca. 2 mm thick) perpendicular to the growth

226   direction. One section of each specimen was glued to a microscope slide with JB KWIK epoxy resin and

227   was later used for geochemical analyses. The other section was used for SEM observations. All shell

228   sections were ground on a Buehler Metaserv 2000 grinder-polisher machine with silicon carbide papers

229   of different grit sizes (P320, P600, P1200, P2500). After each grinding step, the slabs were immersed in

230   de-ionized water and ultrasonically rinsed for 2 minutes. A Buehler VerduTex cloth with a 3 μm

231   diamond suspension was used to polish the sections. The sections used for SEM analysis were etched for

232   5 s in 1 vol% HCl and bleached for 30 min in 6 vol% NaOCl, to remove the organic sheets masking the

233   microstructures.

234

235

236   ## 2.6 Macro-, microstructural and mineralogical analyses

237   Modern shells were photographed before and after the thermal treatments allowing a visual comparison

238   at macroscopic scale. To identify thermal changes, the coloration of the shells was identified according

239   to the Pantone colour system. The sections prepared for the SEM were analysed using a Zeiss Axio

240   Imager.A1m stereomicroscope to record potential changes in the appearance of the two shell layers.

241   Prior to the microstructural analysis, the samples were sputter-coated with a 2 nm-thick layer of

242   platinum using a Leica EM ACE200 Vacuum Coater. The surface of the sections was studied with a 3rd

243   generation LOT Quantum Design Phenom Pro desktop SEM with 10 kV accelerating voltage equipped

244   with a backscatter electron detector. Shell mineralogy was investigated in each shell layer by using a

245   Horiba Jobin Yvon LabRam800 spectrometer equipped with an Olympus BX41 optical microscope. The

246   instrument employed a 532.21 nm laser wavelength, a 400 μm confocal hole, a grating with 1800

247   grooves/mm, an entrance slit width of 100 μm and 50× long-distance objective lens. The integration

248   time of each scan ranged between 3 and 5 s.

249

250

251   2.7 Stable isotope analysis

252   The stable isotope composition of the modern specimens was analysed on carbonate powder sampled

253   after heating the shells. Carbonate material was obtained from each shell by microdrilling the inner layer

254   (nacre) with a Rexim Minimo dental drill mounted to a stereomicroscope and equipped with a conical

255   drill bit of 300 μm in diameter (Komet/Gebr. Brasseler GmbH & Co. KG, model no. H52 104 003). A

256   Thermo Fisher MAT 253 gas source isotope ratio mass spectrometer in continuous flow mode coupled

257   to a GasBench II at the Institute of Geosciences, University of Mainz was used to analyse the carbonate

258   samples by phosphoric acid digestion (70 °C for 120 min). The isotope data were calibrated against a

259   NBS-19 calibrated Carrara marble standard ($\delta^{18}O$ = - 1.91 ‰). The average internal precision (1σ) was

260 0.03‰ and the external reproducibility (1σ) was 0.05‰. The $\delta^{18}O$ profiles of the heated shells were

261 compared to the $\delta^{18}O$ profiles of the control specimens, which were not exposed to high-temperature

262 treatments.

263

264

265 2.8 Radiocarbon dating

266 For radiocarbon dating, small chips were taken near the apex of three *P. turbinatus* specimens. In order

267 to avoid any contamination from sedimentary calcium carbonate or a mixture of different shell layers,

268 the external layer of the shells was physically removed. The fragments of nacre were further processed

269 at the Curt-Engelhorn-Center for Archaeometry, Mannheim, Germany. The material was acidified in

270 phosphoric acid at 70 °C by using an Autosampler system and measured using the MICADAS system

271 (Kromer et al., 2013; Wacker et al., 2013). The results were calibrated with the Marine13 curve (Reimer

272 et al., 2013) and corrected using the Mediterranean reservoir correction (ΔR) of 58 ± 85 ^{14}C years

273 (Reimer and McCormac, 2002) using OxCal v.4.3.2.

274

275

276 2.9 Statistical analyses

277 ANOVA, Mann-Whitney and Tukey´s HSD post hoc tests were performed using the software PAST to

278 test whether the 5-minute heat exposure had a significant effect on shell geochemistry as well as whether

279 the different durations changed the oxygen isotopic signatures.

280

281

282

3. Results

3.1 Experimental results on the effect of roasting on the shells

At macroscopic level, the 5-minute thermal treatment caused a similar effect as reported for *P. turbinatus* in the previous experiment by Milano et al. (2016), in which shells were roasted for 20 minutes and 60 minutes. Visible alteration of the shell surface occurred at temperatures higher than 200 °C. For instance, the typical background cream coloration (Pantone: 7497 C) alternated with pigmented blotches (438 C) started to change at 300 °C, when the shells acquired a dark coloration with a tendency toward a brown shade (background: 7531 C; blotches: 7518 C). At 400 and 500 °C, the shells became grey (background: 404 C; blotches: 417 C) and the outer shell layer started to detach. At 600 °C, the coloration only slightly changed (background: 416 C; blotches: 417 C) and the material brittleness increased, whereas at 700 °C, the coloration turned into a cream-white tone (background and blotches: 401 C; Fig. 2A). Furthermore, the heat exposure induced a 14 to 25% weight loss, with a greater loss at higher temperatures (Fig. 2B).

At the microstructural level, roasting at 200 °C did not cause any visible change of the shell microstructure. First-order and second-order prisms (oSL) and platelets (iSL) of the heated samples did not appreciably differ from those of unheated samples. At 300 °C, the oSL did not show any visible alteration whereas the nacre platelets became slightly porous with nanometer sized holes appearing on their surfaces (Fig. 2C-D). At 400 °C, the single second-order prisms of the oSL were still recognizable. However, sheets of organic material emerged between the first-order prisms partially covering the shell surface. The platelets of the nacre started to fuse and large cracks developed on the surface. After heating at 500 °C, the oSL underwent a significant transformation with the formation of new irregular-shaped units surrounded by organic sheets. Meanwhile, the iSL surface was partially covered by organic

306   matter which emerged from the inter-lamellar voids that formed at 400 °C (Fig. 2C-D). The appearance

307   of the oSL at 600 °C is very similar to the previous treatment (500 °C) with an enhanced presence of

308   organic material. The platelets of the nacre showed a higher degree of fusion in every direction with

309   large quantities of organics in between them. At 700 °C, the surface of the biomineral units of the oSL

310   units became more compact with a decrease in porosity. At the same time, the agglomeration of the iSL

311   platelets led to the formation of new boundaries delineating larger and irregular units (Fig. 2C-D).

312

313   The shell mineralogy was also affected by heat (Fig. 2C-D). Originally, the shells were fully

314   aragonitic as indicated by Raman peaks at 152 cm^{-1},180 cm^{-1}, 207 cm^{-1},707 cm^{-1}and 1086 cm^{-1}. The

315   transition from aragonite into calcite started at 400 °C in the oSL and is indicated by an extra peak at

316   281 cm^{-1} (Fig. 2C). At this temperature, however, the iSL was still completely aragonitic. At 500 °C,

317   both layers were transformed into calcite with peaks at 153 cm^{-1}, 281 cm^{-1}, 713 cm^{-1} and 1086 cm^{-1}.

318

319   Similar to our previous results (Milano et al. 2016), the shell oxygen isotope composition changed

320   in response to the heat treatment. The $\delta^{18}O_{shell}$ values of the control sample ranged between - 1.0 and +

321   1.0 ‰. The oxygen isotope range is more negative than the range obtained by the control shells used in

322   Milano et al. (2016). This offset reflects the difference of the local environments. The shells from

323   Portugal used in the present study were collected from an area characterized by much larger freshwater

324   input, and hence lower $\delta^{18}O_{shell}$ values, than the specimens from Libya used in Milano et al. (2016). The

325   oxygen isotope composition of shells processed at 200 °C and 300 °C for 5 mins ranged between - 0.5

326   and + 0.7 ‰ (Fig. 3A). According to the Mann-Whitney u-test there is no statistical difference between

327   these heated samples and the control shells (p > 0.05; Fig. 3B). The effect of the shell exposure at 400

328   °C could not be tested, because the nacre layer was too thin to obtain sufficient carbonate powder. As

329   expected, higher temperatures (500 - 700 °C) had a significant influence on $\delta^{18}O_{shell.}$ Average values

330   were offset by -1.5 ‰ ± 0.2 with respect to the average values of the control material. Minimum and

331   maximum values were offset by -0.8 ‰ ± 0.1 and -0.8 ‰ ± 0.7, respectively (Fig. 3A). The oxygen

332   isotopic composition of the shells heated over 500 °C was statistically different from the lower

333   temperature treatments and the control conditions (Mann-Whitney test p < 0.05; Fig. 3B). A comparison

334   between the current data and the results published in Milano et al. (2016) was used to determine the

335   influence of the duration of the heating process on the shell. The offsets of the $\delta^{18}O_{shell}$ values from the

336   respective control values were calculated for the three duration treatments (5, 20 and 60 min). The

337   offsets of minimum, average and maximum $\delta^{18}O_{shell}$ values were statistically similar among all treatment

338   durations (ANOVA p > 0.05).

339

340

341   3.3 Archaeological shells: structural and mineralogical organization

342   The *P. turbinatus* specimens from the Haua Fteah presented inter-individual differences in their

343   appearance at macroscopic scale (Fig. 4). All of the Mesolithic specimens (Trench M) showed a

344   homogenous dark grey surface with areas of partial detachment of the oSL (i.e. M002_1 in Fig. 4D,

345   Supplementary material Fig. S1). The nacre was less uniform and lighter grey in colour. In general,

346   these shells looked similar to those of the experiment roasted at 600 °C (Fig. 2A). Two specimens from

347   the Neolithic context 747 (U747_1 and U747_2) were lighter grey and looked similar to shells heated at

348   500 °C (Supplementary material Fig. S1). The third specimen from this layer (U747_3) showed an

349   iridescent iSL and an overall coloration likely related to lower heating temperatures (i.e., 300 °C;

350   Supplementary material Fig. S1). All four Neolithic *P. turbinatus* specimens from context 743 were

351   light brown in colour and showed iridescent nacre (i.e. U743_3 in Fig. 4B). The same applied to the two

352   shells from context 742 (U742_2 and U742_4; Fig. 4A, Supplementary material Fig. S1), whereas

353   U742_1 and U742_3 were grey as if subjected to higher temperatures (Fig. 4C, Supplementary material

354   Fig. S1).

355

356   In good agreement with the observations of the macro appearance of the shells, microstructures

357   varied greatly between individuals. The prisms in the oSLs of the Mesolithic specimens from were

358   replaced by porous irregular units and the nacre platelets were fused together into larger agglomerates

359   (Fig. 4D, Supplementary material Fig. S2). The integral microstructural reorganization and the

360   subsequent absence of any of original secondary prisms (oSL) and platelets (iSL) recall the structural

361   arrangement of the modern samples exposed to high temperatures (600 °C; Tab. 2). A similar

362   architecture was observed in the Neolithic specimens U747_1, U747_2 and U742_3. On the other hand,

363   all shells from context 743 and specimens U747_3 and U742_4 showed well-defined prismatic

364   structures in the oSL and slightly porous platelets in the iSL, which looked similar to the experimental

365   shells heated at 300 °C (Fig. 4B, Supplementary material Fig. S2). Shell U742_1 represented the only

366   case identifiable as processed at a temperature of ca. 500 °C (Table 2). The prisms of the oSL appeared

367   to have undergone major fusion at 400 °C (Fig. 4C). However, the single elongated prisms were still

368   partially visible and they were not completely transformed as in the case of the material burned at 600

369   °C. A similar pattern was observed in the nacre, where the agglomerations of platelets started to define

370   new structural units (Fig. 4C). The microstructures of specimen U742_2 were perfectly preserved and

371   did not show any sign of thermal alteration (Fig. 4A, Table 2).

372

373   According to Raman spectroscopy, seven shells were entirely aragonitic and eleven were calcitic

374   (Fig. 5). All Mesolithic specimens and four of the Neolithic specimens consisted of calcite (Fig. 5A),

375   whereas the remaining specimens from Trench U were aragonitic (Fig. 5B). No transition phase was

376   detected and the two shell layers always shared the same mineralogy. Based on the results presented

377   above, the calcitic shells were categorized as having been exposed to temperatures in excess of 500 °C

378   (Tab. 2).

379

380   Similar to the *P. turbinatus*, some archaeological specimens of *A. uropigimelana* and *T. palustris*

381   from the United Arab Emirates sites displayed an altered overall appearance (Fig. 6). Shells K4 SL

382   Ana3, KSM UBL Ana2, KK1 Ana3 and KK1 Ana4 showed the characteristic homogenous creamy

383   colour of unaltered *A. uropigimelana* (Fig. 6A; Supplementary material Fig. S3). A slightly darker

384   shade, especially on the inner shell surface, was visible in KK1 Ana4. Two shells, KS Ana1 and K4 SL

385   GA1, showed a grey shell surface. The first was characterized by a light tone, whereas the latter was

386   darker with shaded areas on the inner shell surface clearly indicating heat exposure (Fig. 6A;

387   Supplementary material Fig. S3). In the case of *T. palustris*, one specimen (K4 BZ UGT 1) had its

388   surface coloration preserved, whereas a second specimen (K4 BZ GT 1) was very dark (Fig. 6B).

389

390   The well-preserved *A. uropigimelana* specimens K4 SL Ana3, KSM UBL Ana2, KS Ana1, KK1

391   Ana3 and KK1 Ana4 showed well-defined crossed-lamellar structures in the oSL, linear-crossed

392   lamellae in the mSL and irregular complex-crossed lamellae in the iSL. The excellent preservation state

393   was also corroborated by the presence of organic microtubules across the shell layers (Fig. 6A;

394   Supplementary material Fig. S3). Conversely, shell K4 SL GA1 displayed altered microstructures. The

395   first order lamellae of the oSL and mSL were still visible, whereas the morphometric characteristics of

396   the third order lamellae were changed. The units were fused together in large agglomerates with new

397   boundaries (Fig. 6A). These features recall the oSL of *Phorcus* spp. heated at 600 °C. In the iSL, the

398 lamellae lost their individuality and elongated shape, forming compact clusters of material separated by

399 organic sheets and cracks (Fig. 6A). The *T. palustris* specimen K4 BZ UGT 1 showed the typical simple

400 and linear-crossed lamellar microstructures (Fig. 6B), whereas in specimen K4 BZ GT 1 lamellar

401 biomineral units were transformed into large irregular-shaped assemblages in the oSL and iSL. In the

402 mSL, small granular carbonate units with well-defined boundaries prevailed (Fig. 6B). Such alteration

403 was likely related to high temperatures ($\geq$ 500 °C). However, in this case an accurate estimate of the

404 processing temperature cannot be provided based on the microstructures, because no such architecture

405 was previously observed in the mSL.

406

407 Typical aragonite Raman spectra occurred in all but two *A. uropigimelana* and *T. palustris*

408 specimens. The mineralogy of K4 SL GA1 and K4 BZ GT 1 was entirely calcitic (Fig. 7A-B).

409

410

411 3.4 Radiocarbon dating of *P. turbinatus* from Haua Fteah

412 Specimen U742_2, with no sign of heat exposure (Fig. 4A), was dated to 7184 $\pm$ 21 ^{14}C yr BP calibrated

413 to 7772 - 7438 cal. BP (2σ). Specimen U742_1, with signs of high temperature exposure (Fig. 4C), was

414 dated to 7300 $\pm$ 21 ^{14}C yr BP calibrated to 7901 - 7556 cal. BP. both these dates fit with existing [14]C

415 dates for context U742. Specimen U742_3 (Fig. 4B), with burning marks, was dated to 6378 $\pm$ 21 ^{14}C yr

416 BP calibrated to 7002 - 6558 cal. BP. These dates fit with the current chronostratraphic understanding of

417 Context U743, which is paired with U742 stratigraphically (Fig. 8). Associated ^{14}C radiocarbon ages are

418 available from other materials dated in Trench U are also included in this study for comparative

419 purposes (Table 3). The relatively broad spread of dates from U742 fits sedimentological model for this

420 part of the Haua Fteah deposition sequence and all sit within the existing age range for these context.

421 Context U742 is one of a group of chronologically identical contexts (with U743, U744, U746 and

422 U747) that form a cross section of a debris flow that contains archaeological material that can be

423 attributed to the Neolithic.

424

425

426

4. Discussion

4.1 A comparative approach to thermal-induced diagenesis in biogenic carbonates

429 Diagenesis encompasses all physical and chemical processes occurring to the tissues after the death of

430 the animal. The present study focuses exclusively on thermally-induced diagenesis associated with heat

431 exposure. High temperatures accelerate a process that naturally would require thousands of years. When

432 dealing with archaeological remains it is important to differentiate between the two types of diagenetic

433 processes to ensure a correct interpretation of the results. In order to do so, the whole shell assemblage

434 needs to be taken into consideration. Specimens from a certain archaeological layer are subjected to

435 similar environmental conditions after burial (i.e. depth, sediment composition and soil pH). Therefore

436 they are likely to share similar preservation conditions. The overall preservation state indicates whether

437 natural diagenesis altered the shells or not. Any deviation from the average preservation state is likely

438 related to different processes. In our case, shells without evidence of burning are generally well-

439 preserved suggesting that natural diagenesis did not occur (Prendergast et al., 2016). Any altered shell is

440 likely to be related to heat-induced diagenesis. Although this approach allows a reasonable distinction

441 between natural and artificial diagenesis, further studies on naturally-altered shell material are needed to

442 characterize the structural and mineralogical key features relative to this type of diagenesis.

443

444   As previously demonstrated by Milano et al. (2016), the macroscopic and microscopic appearance

445   of *Phorcus* spp. shells gradually altered as the processing temperatures increased. Although the thermal

446   exposure time was reduced to 5 minutes in the present study, similar mineralogical and geochemical

447   changes were observed. The only exception is the temperature at which the aragonite-to-calcite

448   transformation of the oSL occurred, i.e., 400 °C in the present study and 300 °C in Milano et al. (2016).

449   Based on this discrepancy, we suggest that the duration of the thermal exposure may play a role in the

450   development rate of such taphonomic processes. However, time is only of secondary importance in

451   comparison to the actual processing temperature. In good agreement with the most of our results,

452   Aldeais et al. (2016) demonstrated that the mineralogy of *Cerastoderma edule* and *Scrobicularia plana*

453   shells showed no differences after roasting for 5 and 20 minutes. In abiogenic and biogenic minerals, the

454   aragonite-to-calcite and microstructural transformations have been previously observed to occur very

455   rapidly at critical temperatures around 400 °C and 500°C, respectively (Lécuyer, 1996; Koga et al.,

456   2013). As a consequence, it will most likely be impossible to reconstruct the processing duration based

457   on the analysis of archaeological shells, but it is possible to reconstruct the temperatures at which they

458   were exposed. Consequently, it may be possible to postulate the type of fire or fuel that created those

459   temperatures.

460

461   *P. lineatus* shells lost weight after roasting, especially at temperatures above 300 °C (21.5 %

462   weight loss). Heat-induced weight losses have previously been reported from biogenic and abiogenic

463   minerals (Yoshioka and Kitano, 1985; Balmain et al., 1999; Bourrat et al., 2007). Thermal exposure

464   induces a three-step release of water and organic content. At first, the endothermic reaction provokes

465   dehydration through evaporation of the water incorporated in the mineral phase (Yoshioka and Kitano,

466   1985; Perić et al., 1996; Huang et al., 2009). Then, at temperatures between 250 °C and 450 °C, the

467   organic matter in the shell starts to degrade (Bourrat et al., 2007; Huang et al., 2009). In *Phorcus* spp.,

468   this temperature range conforms to the appearance of large organic sheets partially masking the

469   carbonate microstructures (Fig. 2). The degradation intensifies at higher temperatures (> 500 °C) and is

470   associated with weight losses up to 50 % (Balmain et al., 1999; Zolotoyabko and Pokroy, 2007; Huang

471   et al., 2009; Villagran et al., 2011).

472

473   In the present study, temperature was increased stepwise by 100 °C steps to systematically

474   investigate structural and mineralogical changes of the shells. The outer shell layer of *P. lineatus* started

475   to transform from aragonite to calcite at 400 °C. This process was completed at 500 °C. In the case of

476   the nacre, no such broad transition phase was detected. Conversion to calcite took place at 500 °C, at

477   which point the iSL was entirely calcitic. According to previous studies, however, polymorphic

478   transition of mollusk shells already started at temperatures of 250 - 350 °C, and conversion to calcite

479   was completed between 400 °C and 500 °C (Lécuyer, 1996; Maritan et al., 2007; Aldeias et al., 2016).

480   Conversion temperatures seem to vary between species. As shown by Aldeias et al. (2016), the

481   mineralogy of *C. edule* and *S. plana* reacts differently to heating. In *C. edule* polymorphic conversion

482   occurs between 250 and 500 °C, whereas in *S. plana* the transformation only starts at 350 °C and is

483   completed at 400 °C. The observed differences in polymorphic conversion temperatures may be

484   explained by specific structural properties of the materials. Crystal morphology and crystallography

485   were previously identified as potential factors controlling mineralogical transformations (Koga et al.,

486   2013). In abiotic systems, aragonite crystals split and released water trapped within them. Furthermore,

487   calcite nucleation occurs preferably along mineral cracks and twin boundaries (Bischoff and Fyfe, 1968;

488   Liu and Yund, 1993). For these reasons, crystal characteristics and positions of boundaries influence the

489   conversion reaction (Koga et al., 2013). The architectural diversity among mollusk species and shell

490   layers may be the origin of the variable reaction of different biominerals to thermal stress (Kobayashi

491   and Samata, 2006). Aragonitic mineral units tend to lose density and acquire nanopores on their

492   surfaces, while a network of cracks forms in the material (Perdikouri et al., 2011; Villagran et al., 2011;

493   Gomez-Villalba et al., 2012). These features were also observed in the present study in *P. lineatus*

494   specimens roasted at 400 °C, i.e., before full conversion into calcite.

495

496   Given the complexity in the thermal behaviour of biogenic materials, the three-pronged approach

497   of mineralogical, macro- and microscopic observations is essential to better understand the thermally-

498   induced diagenetic processes. The identification of specific changes in the shell can be used as indicator

499   of shell processing temperatures, although possibly with some differences from species to species.

500

501

502   4.2 Implications of heat exposure for palaeoenvironmental reconstructions

503   Heat exposure can induce an exchange of oxygen isotopes with the surrounding environment, drastically

504   altering initial shell isotopic composition (Andrus and Crowe, 2002; Milano et al., 2016). Temperatures

505   higher than 300 °C are observed to cause a significant decrease in $\delta^{18}O_{shell}$ (Milano et al., 2016). Our

506   results are in good agreement with the previous findings suggesting that the use of burnt mollusk shells

507   may have important implications for palaeoenvironmental reconstructions. A decrease in $\delta^{18}O_{shell}$

508   translates into an overestimation of the reconstructed water temperature, which can jeopardize the

509   reliability of related reconstructions. Furthermore, burning at high temperatures can influence the results

510   of palaeoseasonality studies by incorrectly estimating the season(s) of mollusk collection, which in turn

511   may affect the interpretation of hunter-gatherer mobility and settlement use.

512

513   It is recommended to discard shells with signs of thermal exposure for isotopic analyses. However,

514   it has to be noted that not all heating intensities imply isotopic alteration. Low temperatures ($< 300\ °C$)

515   do not induce significant changes in the $\delta^{18}O_{shell}$. Shells exposed to such temperatures can still be used to

516   accurately estimate palaeotemperatures. However, a careful analysis is needed to differentiate between

517   the different heat exposures and to ensure an optimal sample selection for isotopic studies. It is also

518   advisable to avoid any form of pre-treatment involving heating, which was commonly adopted in the

519   past as method for organic matter removal (Mook, 1971).

520

521

522   ## 4.3 Prehistoric fire events and shell middens

523   Different types of fire events can be associated to shell middens, according to their nature and use. The

524   first evidence for controlled fire is dated to around 300,000-250,000 years ago and it is related to a

525   change in hominin habits, especially concerning diet (James et al., 1989; Shahack-Gross et al., 2014;

526   Gowlett, 2016). Among the main benefits of using fire for dietary purposes are the maximization of

527   energy gain and food digestibility and the development of social abilities such as storing, sharing and

528   processing food (Ragir, 2000; Wrangham and Conklin-Brittain, 2003; Wrangham, 2009; Wrangham and

529   Carmody, 2010). Several ethnographic studies suggest that cooking may play an important role in

530   shellfish consumption (Percy, 1608; Meehan, 1977, 1982). Cooking is generally known to facilitate the

531   extraction of the edible portion. In fact, the heat weakens the muscle attachment of the mollusks causing

532   the valves to open (bivalves) and the flesh to detach more easily. In Australia and North America

533   mollusks were placed over or underneath fire, coals or hot stones (Kroeber and Barrett, 1960;

534   Beaglehole, 1974; Bailey, 1977). In other cases, they were cooked in earth ovens (Meehan, 1982;

535   Waselkov, 1987; Thoms, 2008). Additionally, steaming was adopted as an alternative technique by

536 some ethnic groups such as the Maori in New Zealand and the Quileute and the Tlingit in the Pacific

537 Northwest (Best, 1924; Reagan, 1934; Newton and Moss, 1984). Generally, the cooking processes were

538 rather fast, possibly lasting only a few minutes (Meehan, 1977; Thoms, 2008). After being cooked,

539 mollusk soft tissues were sometimes dried or smoked to enable storage for longer periods of time and

540 for trading purposes (Greengo, 1952; Moss, 1993). In addition to food preparation, fire could have being

541 used for trash disposal (Ford, 1989). Ethnographic observations by Meehan (1982) describe occasional

542 burning of food debris by igniting grass on top of large mounds of disposed shells. However, in other

543 cases, the shells were arranged in heaps and covered with sand, without involving any fire (Bird and

544 Bird, 1997). Alternatively, Mougne et al. (2014) suggested the shell refuses to be directly thrown into a

545 fire.

546 To contextualize our results in the light of the ethnographic records, the experimental work by

547 Aldeias et al. (2016) simulating different firing techniques offers a valuable source of information. The

548 authors showed that when a fire was set on top or underneath a pile of shells, there was a great degree of

549 heterogeneity in the shell mineralogical response. The heat diffusion affected differently the single

550 specimens according to their position in respect to the heat source, resulting in a mixture of aragonitic

551 and calcitic shells. Our results indicate that the distribution of specific burning-related features is

552 generally shared among the specimens of the same layer suggesting a homogenous exposure to heat. An

553 exception to this trend is represented by the shells from the Neolithic layer U742, which will be

554 discussed further below. Such uniform heat exposure likely implies heating of relatively small quantities

555 of shells with a similar position in respect to the fire whereas large amounts of material, characteristic of

556 disposal mounds, would induce a significant spatial heat gradient and diverse thermal response.

557 Furthermore, concerning the food disposal by throwing the shells into the fire, this involves direct

558 contact with extreme temperatures. Under these circumstances, the shells would become extremely

559 brittle and prone to a rapid disintegration with limited chances of fossil 'survival' (Milano et al., 2016).

560 In this perspective, our data conform better with firing events associated to food processing rather than

561 food disposal. However, further analysis on additional material is needed before unequivocally

562 discriminate between the two different types of fire.

563

564   Estimation of shellfish heating temperatures from the Haua Fteah suggests a clear distinction

565 between the two archaeological contexts studied here. The seven Mesolithic shells all appear to have

566 been exposed to temperatures between 600 and 700 °C. These temperatures can be reached when the

567 shellfish are situated in close proximity to the heat source without being directly in contact with it.

568 Temperatures between 633 and 781 °C were recorded when experimentally roasting the mollusks on a

569 surface with fuel and fire on top of them (Aldeias et al., 2016). Such temperatures fit well with our

570 observations on the shell remains. However, it has to be considered that roasting temperatures also

571 largely depend on the type of fuel used. In the experiments by Aldeias et al. (2016), pine wood and pine

572 needles were adopted, whereas grass material is known to burn at lower temperatures (max. 430 °C;

573 Wolf et al., 2013). In the light of these observations and our own results, shellfish during the Mesolithic

574 phase at the Haua Fteah were probably processed underneath woody fires.

575

576   In contrast, the Neolithic shells from the Haua Fteah layers U747 and U743 have features pointing

577 to lower temperature exposure: ca 71 % were heated at temperatures around 300 °C. The drastic increase

578 in remains exposed to lower temperatures in the Neolithic phase can be explained by changes in the

579 shellfish processing. A potential interpretation is related to the appearance of the first pottery during the

580 Neolithic, which could have been used to prepare shellfish (McBurney, 1967; Douka et al., 2014;

581 Prendergast et al., 2016). Although the use of vessels for processing marine resources has not been yet

582   attested around the Mediterranean during the Neolithic (Debono Spiteri and Craig, 2014), it has been

583   previously observed in other regions (Craig et al., 2011; Taché and Craig, 2015).   An experiment

584   conducted by Maggetti et al. (2011) showed that clay pots exposed to fire can reach temperatures of

585   around 300 °C after ca. 10 minutes, supporting our observations in the shells of layers U747 and U743.

586   A second interpretation of the lower temperature exposure during the Neolithic encompasses similar

587   heating processes with the adoption of substantially different types of fuel. As mentioned above, the

588   usage of grasses as fuel could explain the lower burning temperatures experienced by the Neolithic

589   shells.

590

591   As an exception to the general trend observed in the results, the shells from unit U742 present

592   heterogeneous burning features related to temperatures from 300 °C to 600 °C, with one shell without

593   any burning sign. On the basis of our observations two hypotheses can be discussed. Different burning

594   degrees may indicate the presence of a thermal gradient related with the use of fire for disposal

595   purposes. Alternatively, the shell may reveal changes in cooking processes in relation to the type of fuel

596   used and/or cooking vessels adoption.

597

598   In the case of the archaeological samples from the United Arab Emirates, both species showed

599   evidences related to heating at 500 - 600 °C. Archaeological sites in this area dated to the late Bronze

600   Age or Classic Wadi Suq period (2000 - 1500 BC) are characterized by a large amount of pottery

601   remains such as beakers and spouted globular jars (Carter, 1997). In this region, food processing with

602   pots seems to have appeared during the Bronze Age, whereas roasting on fire was the preferred method

603   in earlier times (Händel, 2013). However, the small sample size considered in the present study does not

604 allow us a more precise interpretation. In order to better understand the evolution of shellfish processing

605 in the area, additional specimens are needed.

606

607 Together with intentional fires, natural burning events can occur in shell middens. A distinction

608 between intentional and unintentional firing events can hardly be determined on the basis of shell

609 thermal response. However, as in the case of disposal by directly throwing the shells into fire, long-

610 lasting uncontrolled fires would lead to the complete disappearance of the shell remains within the

611 midden. In our case, the preservation of large fragments and whole shells suggests that the heat exposure

612 was likely not related to long-lasting natural fires. However, rapid fires cannot fully be discharge as

613 potential burning sources.

614

615

616 4.4 Heat exposure and radiocarbon dating robustness

617 Previous studies on shell-tempered pottery showed that these materials provide consistent $^{14}C_{AMS}$

618 dates (Rick and Lowery, 2013). To obtain resistant ceramics, shell-tempered pottery is typically fired at

619 300 - 600 °C and - after cooling - fired again to 500 - 600 °C (Kingery et al., 1976; Herbert, 2008). Such

620 temperatures do not seem to affect radiocarbon ages on the shell inclusions, which fit well with dates

621 from charcoal and bone fragments of the same context (Rick and Lowery, 2013). Shells analysed in the

622 present study did not differ from already available ages of the same stratigraphic context. According to

623 the structural and mineralogical analyses, two of the samples were burned at 500 °C and 600 °C,

624 whereas the third one was not burned. The relatively homogeneous AMS dates suggest that heating does

625 not affect radiocarbon ages, even when polymorphic transformation has occurred. This may be due to

626 the fact that the extremely small quantity of carbon remaining in the material (ca 0.1 wt%) is still

627 enough to allow AMS dating (Lanting et al., 2001). Furthermore, physical alterations of the biomineral

628 such as structural unit enlargement and recrystallization seem to provide a barrier protecting the

629 remaining carbon (van Strydonck et al., 2005).

630

631

632 4.5 Methods to identify thermal exposure on shell remains

633 Our results show that the overall appearance of shells alone is an insufficient approach to identify

634 heating-related changes (Milano et al., 2016). Although useful in cases of exposure to high temperatures

635 with evident burning marks, examination by the naked eye has important limitations when it comes to

636 lower temperatures. For instance, based on the outer shell layer, specimen U742_2 seemed to have been

637 exposed to 300 °C. However, according to more detailed analysis using SEM it turned out to be

638 untreated.

639   The analysis of the mineralogical response to heat is valuable when combined with other methods.

640 However, it may prove ambiguous when used alone. The archaeological material analyzed for this study

641 did not show any carbonate polymorph transition phase. Therefore, Raman spectroscopy could only help

642 to distinguish between temperatures below and above 500 °C. Our current and previous results indicate

643 that a combined approach of optical microscopy, SEM and Raman spectroscopy is the most suitable

644 solution to identify alterations related to shellfish processing. The combined use to these techniques will

645 provide more robust data on heating exposure, whether the aim of the research is to preclude heated

646 shells for palaeotemperature reconstructions (Milano et al., 2016) or to examine the food processing in

647 more detail. Although the experimental phase was specifically designed for *Phorcus* spp., the

648 observations showed similarities with the thermal behaviour of *A. uropigimelana* and *T. palustris*. Such

649 analogy in the responses to heat suggests that temperature estimation can be achieved among different

650 mollusk species even without a specific foregoing experimental phase. Results of our findings can be

651 used to answer a broad spectrum of different questions in the framework of shell midden research and

652 shell-tempered pottery studies. Further studies on calcite mollusk shells are needed to complement the

653 existing data on aragonite shells. This will improve the understanding of the biomineralized tissue

654 thermal response in the case of a more stable calcium carbonate phase.

655   Although the methodology developed offers a powerful toolbox to reconstruct shell thermal

656 exposure, care must be paid when interpreting the results in the archaeological context. As discussed, the

657 preservation conditions of the shells (i.e., entire shells/small fragments; homogenous/heterogeneous

658 burning features) can offer insights into the type of fire event. However, these parameters cannot resolve

659 with certainty the exact nature of the fire (intentional/natural; cooking-related/disposal-related).

660 Furthermore, it is important to mention that, given the irreversible nature of the structural and

661 mineralogical thermal response, multiple burning events cannot be discerned. As for any study on burnt

662 remains, the signature preserved is related to the highest temperature experienced by the shell material.

663

664

665

666 ## 5. Conclusions

667   The experimental component of this study has confirmed that shellfish processing methods

668 encompassing temperatures greater than or equal to 300 °C do significantly alter mollusk shell material,

669 but that the duration of the heating does not appear to significantly affect the behaviour of the shell to

670 thermal treatment. According to these findings, structural and chemical changes occur as soon as the

671 shell is exposed to high temperatures. The results also confirm that using burnt shells for

672 palaeoenvironmental reconstructions can produce incorrect temperature estimations and affect the

673 interpretation of environmental and human-related conditions. One proviso to these findings is that the

674 experiments were conducted on fresh shell from which the flesh had been removed when the live

675 mollusks were collected, and further experimental work is needed to establish what impact the presence

676 of body fluids might have on the results. However, burned shells remain a valuable source of

677 information. The experimental changes observed in the modern shells at macro-, microstructural and

678 mineralogical scales have allowed us to determine a set of criteria to detect heating temperatures that can

679 easily be applied to archaeological shells. Analysis of archaeological shells of *P. turbinatus* from the

680 Haua Fteah cave in coastal northeast Libya revealed that during the Mesolithic the shells were uniformly

681 exposed to high temperatures (shells in close proximity to the heat source) whereas during the Neolithic

682 lower temperatures were recorded. Although, the use of fire for non-dietary purposes cannot be

683 completely ruled out, the trend in our results can be interpreted as a temporal change in shellfish

684 preparation.

685 Analysis of archaeological shells of *A. uropigimelana* and *T.palustris* from Neolithic and Bronze

686 Age shell midden sites on the coast of the United Arab Emirates found that some specimens did not

687 show any evidence of burning while others showed indications of high-temperature exposure. Although

688 burning affected the shell structure and mineralogy, it does not appear to have a significant influence on

689 radiocarbon ages suggesting the possibility of using burnt remains for dating purposes. The fact that the

690 thermal reaction of different species is similar provides confidence in applying the techniques outlined

691 in this study at an interspecific level.

692

693

694

695 Acknowledgements

References

Aldeias, V., Gur-Arieh, S., Maria, R., Monteiro, P., Cura, P., 2016. Shell we cook it? An experimental approach to the microarchaeological record of shellfish roasting. Archaeol. Anthropol. Sci. doi:10.1007/s12520-016-0413-1

Andrus, C.F.T., 2011. Shell midden sclerochronology. Quat. Sci. Rev. 30, 2892-2905. doi:10.1016/j.quascirev.2011.07.016

Andrus, C.F.T., Crowe, D.E., 2002. Alteration of otolith aragonite: Effects of prehistoric cooking methods on otolith chemistry. J. Archaeol. Sci. 29, 291-299. doi:10.1006/jasc.2001.0694

Bailey, G.N., 1977. Shell mounds, shell middens, and raised beaches in the Cape York Peninsula. Mankind 11, 132-143.

717   Balmain, J., Hannoyer, B., Lopez, E., 1999. Fourier transform infrared spectroscopy (FTIR) and XRD

718   analyses of mineral and organic matrix during heating of mother of pearl (nacre) from the shell of

719   the mollusc *Pinctada maxima*. J. Biomed. Mater. Res. 48, 749-754. doi:10.1002/(SICI)1097-

720   4636(1999)48

721   Barker, G., Bennett, P., Farr, L., Hill, E., Hunt, C., Lucarini, G., Morales, J., Mutri, G., Prendergast,

722   A.L., Pryor, A., Rabett, R., Reynolds, T., Spry-Marques, P., Twati, M., 2012. The Cyrenaican

723   Prehistory Project 2012: the fifth season of investigations of the Haua Fteah cave. Libyan Stud. 43,

724   115-136. doi:10.1017/S026371890000008X

725   Beaglehole, J.C., 1974 (ed.), The Journals of Captain James Cook on his Voyages of Discovery: The

726   Voyage of the Endeavor, 1768-1771. Hakluyt Society, Cambridge.

727   Beech, M., Kallweit, H., 2001. A note on the archaeological and environmental remains from site JH57,

728   a 5th-4th millennium BC shell midden in Jazirat al-Hamra, Ra´s al-Khaimah. Tribulus 11, 17-20.

729   Berna, F., Goldberg, P., 2008. Assessing Paleolithic pyrotechnology and associated hominin behaviour

730   in Israel. Isr. J. Earth Sci. 56, 107-121. doi:10.1560/IJES.56.2-4.107

731   Best, E., 1924. The Maori. Volume 2. Wellington

732   Biagi, P., Torke, W., Tosi, M., Uerpmann, H., 1984. Qurum : a case study of coastal archaeology in

733   Northern Oman. Coast. Archaeol. 16, 43-61.

734   Bird, D.W., Bliege Bird, R.L., 1997. Contemporary shellfish gathering strategies among the Meriam of

735   the Torres Strait Islands, Australia: Testing predictions of a central place foraging model. J.

736   Archaeol. Sci. 24, 39–63. https://doi.org/10.1006/jasc.1995.0095

737 Bischoff, J.L., Fyfe, W.S., 1968. Catalysis, inhibition, and the calcite-aragonite problem: I. The calcite-

738   aragonite transformation. Am. J. Sci. doi:10.2475/ajs.266.2.80

739 Bosch, M.D., Wesselingh, F.P., Mannino, M.A., 2015. The Ksâr 'Akil (Lebanon) mollusc assemblage:

740   Zooarchaeological and taphonomic investigations. Quat. Int. 390, 85-101.

741   doi:10.1016/j.quaint.2015.07.004

742 Bourrat, X., Francke, L., Lopez, E., Rousseau, M., Stempfle, P., Angellier, M., Alberic, P., 2007. Nacre

743   biocrystal thermal behaviour. R. Soc. Chem. 9, 1205-1208. doi:10.1039/b709388h

744 Broadhurst, C.L., Wang, Y., Crawford, M.A., Cunnane, S.C., Parkington, J.E., Schmidt, W.F., 2002.

745   Brain-specific lipids from marine, lacustrine, or terrestrial food resources: Potential impact on early

746   African *Homo sapiens*. Comp. Biochem. Physiol. - B Biochem. Mol. Biol. 131, 653-673.

747   doi:10.1016/S1096-4959(02)00002-7

748 Burchell, M., Cannon, A., Hallmann, N., Schwarcz, H.P., Schöne, B.R., 2013. Refining estimates for the

749   season of shellfish collection on the Pacific Northwest coast: Applying high-resolution stable

750   oxygen isotope analysis and sclerochronology. Archaeometry 55, 258-276. doi:10.1111/j.1475-

751   4754.2012.00684.x

752 Butler, P.G., Wanamaker, A.D., Scourse, J.D., Richardson, C.A., Reynolds, D.J., 2013. Variability of

753   marine climate on the North Icelandic Shelf in a 1357-year proxy archive based on growth

754   increments in the bivalve *Arctica Islandica*. Palaeogeogr. Palaeoclimatol. Palaeoecol. 373, 141-

755   151. doi:10.1016/j.palaeo.2012.01.016

756 Carlen, A., Olafsson, E., 2002. The effects of the gastropod *Terebralia palustris* on infaunal
757   communities in a tropical tidal mud-flat in East Africa. Wetl. Ecol. Manag. 10, 303-311.

758 Carter, R., 1997. The Wadi Suq period in south-east Arabia: a reappraisal in the light of excavations at
759   Kalba, UAE. Proc. Semin. Arab. Stud. 27, 87-98.

760 Carter, J.G., Harries, P.J., Malchus, N., Sartori, A.F., Anderson, L.C., Bieler, R., Bogan, A.E., Coan,
761   E.V., Cope, J.C.W., Cragg, S.M., Garcia-March, J.R., Hylleberg, J., Kelley, P., Kleemann, K., Kriz,
762   J., McRoberts, C., Mikkelsen, P.M., Pojeta, J.J., Temkin, I., Yancey, T., Zieritz, A., 2012.
763   Illustrated glossary of the bivalvia. Treatise Online 1, 209.

764 Colonese, A.C., Troelstra, S., Ziveri, P., Martini, F., Lo Vetro, D., Tommasini, S., 2009. Mesolithic
765   shellfish exploitation in SW Italy: seasonal evidence from the oxygen isotopic composition of
766   *Osilinus turbinatus* shells. J. Archaeol. Sci. 36, 1935-1944. doi:10.1016/j.jas.2009.04.021

767 Colonese, A.C., Mannino, M.A., Bar-Yosef Mayer, D.E., Fa, D.A., Finlayson, J.C., Lubell, D., Stiner,
768   M.C., 2011. Marine mollusc exploitation in Mediterranean prehistory: An overview. Quat. Int. 239,
769   86-103. doi:10.1016/j.quaint.2010.09.001

770 Craig, O.E., Steele, V.L., Fischer, A., Hartz, S., Andersen, S.H., Donohoe, P., Glykou, A., Saul, H.,
771   Jones, M.D., Koch, E., Heron, C.P., 2011. Ancient lipids reveal continuity in culinary practices
772   across the transition to agriculture in Northern Europe. Proc. Natl. Acad. Sci. U. S. A. 108, 17910-
773   17915. doi:10.1073/pnas.0913714

774 Da Costa, M.A., 2015. Distribution and Shape Analysis of *Phorcus lineatus* and *Phorcus sauciatus*
775   along the Portuguese Coast, Universidade de Lisboa.

776   de Lumley, H., 1966. Les fouilles de Terra Amata à Nice. Premiers résultats. Bulletin du Musée
777   d'Anthropologie et Préhistoire de Monaco 13, 29-51.

778   Debono Spiteri C., Craig, O.E., 2014. Biomolecular and isotopic characterisation of lipid residues
779   absorbed in Impressed Wares from the Early Neolithic village of Skorba, Malta. Malta Archaeol.
780   Rev. 14-22.

781   Donald, K.M., Preston, J., Williams, S.T., Reid, D.G., Winter, D., Alvarez, R., Buge, B., Hawkins, S.J.,
782   Templado, J., Spencer, H.G., 2012. Phylogenetic relationships elucidate colonization patterns in the
783   intertidal grazers *Osilinus* Philippi, 1847 and *Phorcus* Risso, 1826 (Gastropoda: Trochidae) in the
784   northeastern Atlantic Ocean and Mediterranean Sea. Mol. Phylogenet. Evol. 62, 35-45.
785   doi:10.1016/j.ympev.2011.09.002

786   Douka, K., Jacobs, Z., Lane, C., Grün, R., Farr, L., Hunt, C., Inglis, R.H., Reynolds, T., Albert, P.,
787   Aubert, M., Cullen, V., Hill, E., Kinsley, L., Roberts, R.G., Tomlinson, E.L., Wulf, S., Barker, G.,
788   2014. The chronostratigraphy of the Haua Fteah cave (Cyrenaica, northeast Libya). J. Hum. Evol.
789   66, 39-63. doi:10.1016/j.jhevol.2013.10.001

790   Eerkens, J.W., Byrd, B.F., Spero, H.J., Fritschi, A.K., 2013. Stable isotope reconstructions of shellfish
791   harvesting seasonality in an estuarine environment: Implications for Late Holocene San Francisco
792   Bay settlement patterns. J. Archaeol. Sci. 40, 2014-2024. doi:10.1016/j.jas.2012.12.018

793   Erlandson, J.M., 2001. The archaeology of aquatic adaptations: paradigm for a new millennium. J.
794   Archaeol. Res. 9, 287-350.

795   Erlandson, J.M., Rick, T.C., Vellanoweth, R.L., Kennett, D.J., 1999. Maritime subsistence at a 9300

796   year old shell midden on Santa Rosa Island, California. J. F. Archaeol. 26, 255-265.

797   doi:10.1179/jfa.1999.26.3.255

798   Fa, D.A., 2008. Effects of tidal amplitude on intertidal resource availability and dispersal pressure in

799   prehistoric human coastal populations: the Mediterranean-Atlantic transition. Quat. Sci. Rev. 27,

800   2194-2209. doi:10.1016/j.quascirev.2008.07.015

801   Farr, L. Lane, R., Abdulazeez, F., Bennett, P., Holman, J., Marasi, A., Prendergast, A., Al- Zweyi, M.,

802   Barker, G., 2014. The Cyrenaican Prehistory Project 2013: the seventh season of excavations in

803   the Haua Fteah cave. Libyan Stud. 45, 163-173.

804   Ferguson, J.E., Henderson, G.M., Fa, D.A., Finlayson, J.C., Charnley, N.R., 2011. Increased seasonality

805   in the Western Mediterranean during the last glacial from limpet shell geochemistry. Earth Planet.

806   Sci. Lett. 308, 325-333. doi:10.1016/j.epsl.2011.05.054

807   Ford, P.J., 1989. Molluscan assemblages from archaeological deposits. Geoarchaeology 4, 157-173.

808   doi:10.1002/gea.3340040205

809   Gardner, A.S., 2005. Marine mollusc shells from two archaeological sites near Al Ain. Tribulus 15.1, 9-

810   12.

811   Girod, A. 2011. Land snails from Late Glacial and Early Holocene Italian sites. Quaternary

812   International 244, 105-116.

813

814   Gomez-Villalba, L.S., Lopez-Arce, P., Alvarez de Buergo, M., Fort, R., 2012. Atomic defects and their

815   relationship to aragonite-calcite transformation in portlandite nanocrystal carbonation. Cryst.

816   Growth Des. 12, 4844-4852.

817   Goodwin, D.H., Flessa, K.W., Schöne, B.R., Dettman, D.L., 2001. Cross-calibration of daily growth

818   increments, stable isotope variation, and temperature in the Gulf of California bivalve mollusk

819   *Chione cortezi*: Implications for palaeoenvironmental analysis. Palaios 16, 387-398.

820   doi:10.1669/0883-1351(2001)016

821   Greengo, R.E., 1952. Shellfish of the California Indians. Kroeber Anthropol. Soc. 7, 63-114.

822   Gutiérrez-Zugasti, I., Garcia-Escarzaga, A., Martin-Chivelet, J., Gonzalez-Morales, M.R., 2015.

823   Determination of sea surface temperatures using oxygen isotope ratios from *Phorcus lineatus* (Da

824   Costa, 1778) in northern Spain: Implications for paleoclimate and archaeological studies. The

825   Holocene 25, 1002-1014. doi:10.1177/0959683615574892

826

827   Hammond, H. 2014. Taphonomic analysis of archaeomalacological assemblages: shell middens on the

828   northern coast of Santa Cruz (Patagonia, Argentina). Intersecciones in Antropologia Suppl. 15 (1).

829

830   Händel, M., 2013. Al-Hamriya - Dynamik einer Muschelhaufenlandschaft in den Vereinigten

831   Arabischen Emiraten. Archaeologia Austriaca, 77-96.

832   Herbert, J.M., 2008. The history and practice of shell tempering in the Middle Atlantic: A useful

833   balance. Southeast. Archaeol. 27, 265-285.

834 Hill E.A., Reimer, P.J., Hunt, C.O., Prendergast, A.L., Barker, G.W., 2017. Radiocarbon ecology of the

835 land snail *Helix melanostoma* in Northeast Libya. Radiocarbon 59, 1-22. doi:

836 10.1017/RDC.2017.49

837 Houbrick, R.S., 1991. Systematic review and functional morphology of the mangrove snails *Terebralia*

838 and *Telescopium* (Potamididae; Prosobranchia). Malacologia 33, 289-338

839 Huang, Z., Li, X., 2009. Nanoscale structural and mechanical characterization of heat treated nacre.

840 Mater. Sci. Eng. C 29, 1803-1807. doi:10.1016/j.msec.2009.02.007

841 Hunt, C.O., Reynolds, T.G., El-Rishi, H., Buzaian, A., Hill, E., Barker, G.W., 2011. Resource pressure

842 and environmental change on the North African littoral: Epipalaeolithic to Roman gastropods from

843 Cyrenaica, Libya. Quat. Int. 244, 15-26. doi:10.1016/j.quaint.2011.04.045

844 James, S.R., Dennell, R.W., Gilbert, A.S., Lewis, H.T., Gowlett, J.A.J., Lynch, T.F., Mcgrew, W.C.,

845 Peters, C.R., Pope, G.G., Stahl, A.B., 1989. Hominid use of fire in the Lower and Middle

846 Pleistocene: A review of the evidence. Curr. Anthropol. 30, 1-26. doi:10.2307/2743299

847 Jones, D.S., 1983. Sclerochronology: Reading the record of the molluscan shell. Am. Sci. 71, 384-391.

848 Kendall, M.A., 1987. The age and structure of some northern populations of the trochid gastropod

849 *Monodonta lineata*. J. Molluscan Stud. 53, 213-222.

850 Kingery, W.D., Bowen, H.K., Uhlmann, D.R.,1976. Introduction to Ceramics. John Willey and Sons,

851 New York.

852   Kobayashi, I., Samata, T., 2006. Bivalve shell structure and organic matrix. Mater. Sci. Eng. C 26, 692-

853   698. doi:10.1016/j.msec.2005.09.101

854   Koga, N., Kasahara, D., Kimura, T., 2013. Aragonite crystal growth and solid-state aragonite-calcite

855   transformation: A physico-geometrical relationship via thermal dehydration of included water.

856   Cryst. Growth Des. 13, 2238-2246. doi:10.1021/cg400350w

857   Kroeber, A.L., Barrett, S.A., 1960. Fishing among the indians of Northwestern California, University of

858   California Anthropological Records.

859   Kromer, B., Lindauer, S., Synal, H., Wacker, L., 2013. A new AMS facility at the Curt-Engelhorn-

860   Centre for Achaeometry, Mannheim, Germany. Nucl. Inst. Methods Phys. Res. B 294, 11-13.

861   doi:10.1016/j.nimb.2012.01.015

862   Lanting, J.N., Aerts-Bijma, A.T., van der Plicht, J., 2001. Dating of cremated bones. Radiocarbon 43,

863   249-254. doi:10.2458/azu_js_rc.v.3946

864   Lécuyer, C., 1996. Effects of heating on the geochemistry of biogenic carbonates. Chem. Geol. 129,

865   173-183. doi:10.1016/0009-2541(96)00005-8

866   Lindauer, S., Marali, S., Schöne, B.R., Uerpmann, H.-P., Kromer, B., Hinderer, M., 2016. Investigating

867   the local reservoir age and stable isotopes of shells from Southeast Arabia. Radiocarbon 1-18.

868   doi:10.1017/RDC.2016.80

869   Lindauer, S., Santos, G.M., Steinhof, A., Yousif, E., Phillips, C., Jasim, S.A., Uerpmann, H.P., Hinderer,

870   M., 2017. The local marine reservoir effect at Kalba (UAE) between the Neolithic and Bronze Age:

871   An indicator of sea level and climate changes. Quat. Geochronol. 42, 105–116.

872   https://doi.org/10.1016/j.quageo.2017.09.003

873   Liu, M.L., Yund, R.A., 1993. Transformation kinetic of polycristalline aragonite to calcite: new

874   experimental data, modelling and implications. Contrib. to Mineral. Petrol. 114, 465-478.

875   doi:10.1007/BF00321751

876   Maggetti, M., Neururer, C., Ramseyer, D., 2011. Temperature evolution inside a pot during

877   experimental surface (bonfire) firing. Appl. Clay Sci. 53, 500-508. doi:10.1016/j.clay.2010.09.013

878   Mannino, M.A., Thomas, K.D., 2001. Intensive Mesolithic exploitation of coastal resources? Evidence

879   from a shell deposit on the Isle of Portland (Southern England) for the impact of human foraging on

880   populations of intertidal rocky shore molluscs. J. Archaeol. Sci. 1101-1114.

881   doi:10.1006/jasc.2001.0658

882   Mannino, M.A., Thomas, K.D., 2002. Depletion of a resource? The impact of prehistoric human

883   foraging on intertidal mollusc communities and its significance for human settlement, mobility and

884   dispersal. World Archaeol. 33, 452-474. doi:10.1080/00438240120107477

885   Mannino, M.A., Spiro, B.F., Thomas, K.D., 2003. Sampling shells for seasonality: oxygen isotope

886   analysis on shell carbonates of the inter-tidal gastropod *Monodonta lineata* (da Costa) from

887   populations across its modern range and from a Mesolithic site in southern Britain. J. Archaeol. Sci.

888   30, 667-679. doi:10.1016/S0305-4403(02)00238-8

889   Mannino, M.A., Thomas, K.D., Leng, M.J., Piperno, M., Tusa, S., Tagliacozzo, A., 2007. Marine

890   resources in the mesolithic and neolithic at the Grotta dell'Uzzo (Sicily): Evidence from isotope

891   analyses of marine shells. Archaeometry 49, 117-133. doi:10.1111/j.1475-4754.2007.00291.x

892   Mannino, M.A., Thomas, K.D., Leng, M.J., Sloane, H.J., 2008. Shell growth and oxygen isotopes in the

893   topshell *Osilinus turbinatus*: resolving past inshore sea surface temperatures. Geo-Marine Lett. 28,

894   309-325. doi:10.1007/s00367-008-0107-5

895   Marean, C.W., Bar-Matthews, M., Bernatchez, J.A., Fisher, E.C., Goldberg, P., Herries, A.I.R., Jacobs,

896   Z., Jerardino, A., Karkanas, P., Minichillo, T., Nilssen, P.J., Thompson, E., Watts, I., Williams,

897   H.M., 2007. Early human use of marine resources and pigment in South Africa during the Middle

898   Pleistocene. Nature 449, 906-909. doi:10.1038/nature06204

899   Maritan, L., Mazzoli, C., Freestone, I., 2007. Modelling changes in mollusc shell internal microstructure

900   during firing: Implications for temperature estimation in shell-bearing pottery. Archaeometry 49,

901   529-541. doi:10.1111/j.1475-4754.2007.00318.x

902   McBurney, C.B.M. (Ed.), 1967. The Haua Fteah (Cyrenaica) and the Stone Age of the South-East

903   Mediterranean. Cambridge University Press, Cambridge.

904   Meehan, B., 1977. Hunters by the seashore. J. Hum. Evol. 6, 363-370.

905   Meehan, B., 1982. Shell Bed to Shell Midden. Australian Institute of Aboriginal Studies, Canberra.

906   Menzies, R., Cohen, Y., Lavie, B., Nevo, E., 1992. Niche adaptation in two marine gastropods,

907   *Monodonta turbiformis* and *M. turbinata*. Bolletino di Zool. 59, 297-302.

908   doi:10.1080/11250009209386685

909 Milano, S., Prendergast, A.L., Schöne, B.R., 2016. Effects of cooking on mollusk shell structure and
910   chemistry: Implications for archeology and palaeoenvironmental reconstruction. J. Archaeol. Sci.
911   Reports 7, 14-26. doi:10.1016/j.jasrep.2016.03.045

912 Milano, S., Schöne, B.R., Witbaard, R., 2017. Changes of shell microstructural characteristics of
913   *Cerastoderma edule* (Bivalvia) - A novel proxy for water temperature. Palaeogeogr.
914   Palaeoclimatol. Palaeoecol. 465, 395-406. doi:10.1016/j.palaeo.2015.09.051

915 Miyaji, T., Tanabe, K., Schöne, B.R., 2007. Environmental controls on daily shell growth of *Phacosoma*
916   *japonicum* (Bivalvia: Veneridae) from Japan. Mar. Ecol. Prog. Ser. 336, 141-150.
917   doi:10.3354/meps336141

918 Mook, W., 1971. Paleotemperatures and chlorinities [CORRECT?] from stable carbon and oxygen
919   isotopes in shell carbonate. Palaeogeogr. Palaeoclimatol. Palaeoecol. 9, 245-263.
920   doi:10.1016/0031-0182(71)90002-2

921 Moss, M.L., 1993. Shellfish, gender, and status on the Northwest coast: reconciling archeological,
922   ethnographic, and ethnohistorical records of the Tlingit. Am. Anthropol. 95, 631-652.
923   doi:10.1525/aa.1993.95.3.02a00050

924 Mougne, C., Dupont, C., Giazzon, D., Quesnel, L., 2014. Shellfish from the Bronze Age Site of Clos des
925   Châtaigniers (Mathieu, Normandy, France). Internet Archaeol. https://doi.org/10.11141/ia.37.5

926 Newton, R., Moss, M., 1984. The Subsistence Lifeway of the Tlingit People: Excerpts of Oral
927   Interviews. USDA Forest Service Alaska Region Report No.179, Juneau.

928   Nishihira, M., Kuniyoshi, M., Shimamura, K., 2002. Size variation in *Terebralia palustris* (Gastropoda:

929   Potamididae) of Iriomote Isl

930   and, southern Japan, and its effect on some population characteristics. Wetl. Ecol. Manag. 10, 243-247.

931   Oschmann, W., 2009. Sclerochronology: Editorial. Int. J. Earth Sci 98, 1-2. doi:10.1007/s00531-008-

932   0403-3

933   Percy, G., 1608. Observations Gathered out of a Discourse of the Plantation of the Southern Colony in

934   Virginia by the English, 1606.

935   Perdikouri, C., Kasioptas, A., Geisler, T., Schmidt, B.C., Putnis, A., 2011. Experimental study of the

936   aragonite to calcite transition in aqueous solution. Geochim. Cosmochim. Acta 75, 6211-6224.

937   doi:10.1016/j.gca.2011.07.045

938   Perić, J., Vučak, M., Krstulović, R., Brečević, L., Kralj, D., 1996. Phase transformation of calcium

939   carbonate polymorphs. Thermochim. Acta 277, 175-186. doi:10.1016/0040-6031(95)02748-3

940   Petchey, F., Ulm, S., David, B., Mcniven, I.J., Asmussen, B., Tomkins, H., Dolby, N., Aplin, K.,

941   Richards, T., Rowe, C., Leavesley, M., 2013. High-resolution radiocarbon dating of marine

942   materials in archaeological contexts : radiocarbon marine reservoir variability between *Anadara,*

943   *Gafrarium, Batissa, Polymesoda* spp. and Echinoidea at Caution Bay, Southern Coastal Papua New

944   Guinea. Archaeol. Anthropol. Sci. 5, 69-80. doi:10.1007/s12520-012-0108-1

945   Phillips, C.S., Mosseri-Marlio, C.E., 2002. Sustaining change: The emerging picture of the Neolithic to

946   Iron Age subsistence economy at Kalba, Sharjah Emirate, UAE, in: Proceedings of the Fifth

947   International Symposium on the Archaeozoology of Southwestern Asia and Adjacent Areas. ARC-

948   Publicaties, Groningen, The Netherlands. EDITOR(S)?

949   Plaziat, J.C., 1984. Mollusk distribution in the mangal. In: Por D, Dor I (eds) Hydrobiology of the

950   mangal: the ecosystem of the mangrove forests. Junk, Boston, pp. 111-143.

951   Prendergast, A.L., Azzopardi, M., O'Connell, T.C., Hunt, C., Barker, G., Stevens, R.E., 2013. Oxygen

952   isotopes from *Phorcus* (*Osilinus*) *turbinatus* shells as a proxy for sea surface temperature in the

953   central Mediterranean: A case study from Malta. Chem. Geol. 345, 77-86.

954   doi:10.1016/j.chemgeo.2013.02.026

955   Prendergast, A.L., Stevens, R.E., O'Connell, T.C., Fadlalak, A., Touati, M., Al-Mzeine, A., Schöne,

956   B.R., Hunt, C.O., Barker, G.W., 2016. Changing patterns of eastern Mediterranean shellfish

957   exploitation in the Late Glacial and Early Holocene : Oxygen isotope evidence from gastropods in

958   Epipaleolithic to Neolithic human occupation layers at the Haua Fteah cave, Libya. Quat. Int. 407,

959   80-93. doi:10.1016/j.quaint.2015.09.035

960   Prendergast, A.L., Schöne, B.R., 2017. Oxygen isotopes from limpet shells: Implications for

961   palaeothermometry and seasonal shellfish foraging studies in the Mediterranean. Palaeogeogr.

962   Palaeoclimatol. Palaeoecol. 484, 33-47. doi:10.1016/j.palaeo.2017.03.007

963   Ragir, S., 2000. Diet and food preparation: Rethinking early hominid behavior. Evol. Anthropol. 9, 153-

964   155. doi:10.1002/1520-6505(2000)9:4<153::AID-EVAN4>3.0.CO;2-D

965   Reagan, A.B., 1934. Various uses of plants by West Coast Indians. Washingt. Hist. Q. 25, 133-137.

966 Reimer, P.J., McCormac, F.G., 2002. Marine radiocarbon reservoir corrections for the Mediterranean
967   and Aegean Seas. Radiocarbon 44, 159-166.

968 Reimer, P.J., Bard, E., Bayliss, A., Beck, J.W., Blackwell, P.G., Bronk, C., Caitlin, R., Hai, E.B.,
969   Edwards, R.L., 2013. Intcal13 and marine13 radiocarbon age calibration curves 0 - 50,000 years cal
970   CP. Radiocarbon 55, 1869-1887. doi:http://doi.org/10.2458/azu_js_rc.55.16947

971 Rick, T.C., Lowery, D.L., 2013. Accelerator mass spectrometry 14C dating and the antiquity of shell-
972   tempered ceramics from the Chesapeake Bay and Middle Atlantic. Am. Antiq. 78, 570-579.

973 Schembri, P.J., Deidun, A., Mallia, A., Mercieca, L., 2005. Rocky shore biotic assemblages of the
974   Maltese Islands (Central Mediterranean): A conservation perspective. J. Coast. Res. 21, 157-166.

975 Schöne, B.R., 2008. The curse of physiology—challenges and opportunities in the interpretation of
976   geochemical data from mollusk shells. Geo-Marine Lett. 28, 269-285. doi:10.1007/s00367-008-
977   0114-6

978 Schöne, B.R., Freyre Castro, A.D., Fiebig, J., Houk, S.D., Oschmann, W., Kröncke, I., 2004. Sea surface
979   water temperatures over the period 1884-1983 reconstructed from oxygen isotope ratios of a
980   bivalve mollusk shell (*Arctica islandica*, southern North Sea). Palaeogeogr. Palaeoclimatol.
981   Palaeoecol. 212, 215-232. doi:10.1016/j.palaeo.2004.05.024

982 Schöne, B.R., Fiebig, J., Pfeiffer, M., Gleß, R., Hickson, J., Johnson, A.L.A., Dreyer, W., Oschmann,
983   W., 2005. Climate records from a bivalved Methuselah (*Arctica islandica*, Mollusca; Iceland).
984   Palaeogeogr. Palaeoclimatol. Palaeoecol. 228, 130-148. doi:10.1016/j.palaeo.2005.03.049

985   Schöne, B.R., Krause, R.A., 2016. Retrospective environmental biomonitoring - Mussel Watch

986   expanded. Glob. Planet. Change 144, 228-251. doi:10.1016/j.gloplacha.2016.08.002

987   Shackleton, N.J., 1973. Oxygen isotope analysis as a means of determining season of occupation of

988   prehistoric midden sites. Archaeometry 15, 133-141. doi:10.1111/j.1475-4754.1973.tb00082.x

989   Smith, D., 1978. Delia Smith's Complete Cookery Course. BBC Publications, London.

990   Steinhardt, J., Butler, P.G., Carroll, M.L., Hartley, J., 2016. The application of long-lived bivalve

991   sclerochronology   in   environmental   baseline   monitoring.   Front.   Mar.   Sci.   3.

992   doi:10.3389/fmars.2016.00176

993   Taché, K., Craig, O.E., 2015. Cooperative harvesting of aquatic resources and the beginning of pottery

994   production in north-eastern North America. Antiquity 89, 177-190. doi:10.15184/aqy.2014.36

995   Taylor, V.K., Barton, R.N.E., Bell, M., Bouzouggar, A., Collcutt, S., Black, S., Hogue, J.T., 2011. The

996   Epipalaeolithic (Iberomaurusian) at Grotte des Pigeons (Taforalt), Morocco: A preliminary study of

997   the land Mollusca. Quat. Int. 244, 5-14. doi:10.1016/j.quaint.2011.04.041

998   Tebano, T., Paulay, G., 2001. Variable recruitment and changing environments create a fluctuating

999   resource: The biology of *Anadara uropigimelana* (Bivalvia: Arcidae) on Tarawa atoll. Atoll Res.

1000   Bull. 488.

1001   Thoms, A. V., 2008. The fire stones carry: Ethnographic records and archaeological expectations for

1002   hot-rock   cookery   in   western   North   America.   J.   Anthropol.   Archaeol.   27,   443-460.

1003   doi:10.1016/j.jaa.2008.07.002

1004   Van Strydonck M., Boudon M., Hoefkens M., D.M.G., 2005. ^{14}C-dating of cremated bones, why does it

1005   work? Lunula. Archaeol. Protohistorica 13, 3-10.

1006   Villagran, X.S., Balbo, A.L., Madella, M., Vila, A., Estevez, J., 2011. Experimental micromorphology

1007   in Tierra del Fuego (Argentina): building a reference collection for the study of shell middens in

1008   cold climates. J. Archaeol. Sci. 38, 588-604. doi:10.1016/j.jas.2010.10.013

1009   Wacker, L., Fülöp, R., Hajdas, I., Molnár, M., Rethemeyer, J., 2013. A novel approach to process

1010   carbonate samples for radiocarbon measurements with helium carrier gas. Nucl. Inst. Methods

1011   Phys. Res. B 294, 214-217. doi:10.1016/j.nimb.2012.08.030

1012   Waselkov, G.A., 1987. Shell gathering and shell midden archaeology. Adv. Archaeol. Method Theory

1013   10, 93-209.

1014   Wolf, M., Lehndorff, E., Wiesenberg, G.L.B., Stockhausen, M., Schwark, L., Amelung, W., 2013.

1015   Towards reconstruction of past fire regimes from geochemical analysis of charcoal. Org. Geochem.

1016   55, 11-21. doi:10.1016/j.orggeochem.2012.11.002

1017   Wrangham, R., 2009. Catching Fire: How Cooking Made Us Human. Basic Books, New York.

1018   Yoshioka, S., Kitano, Y., 1985. Transformation of aragonite to calcite through heating. Geochem. J. 19,
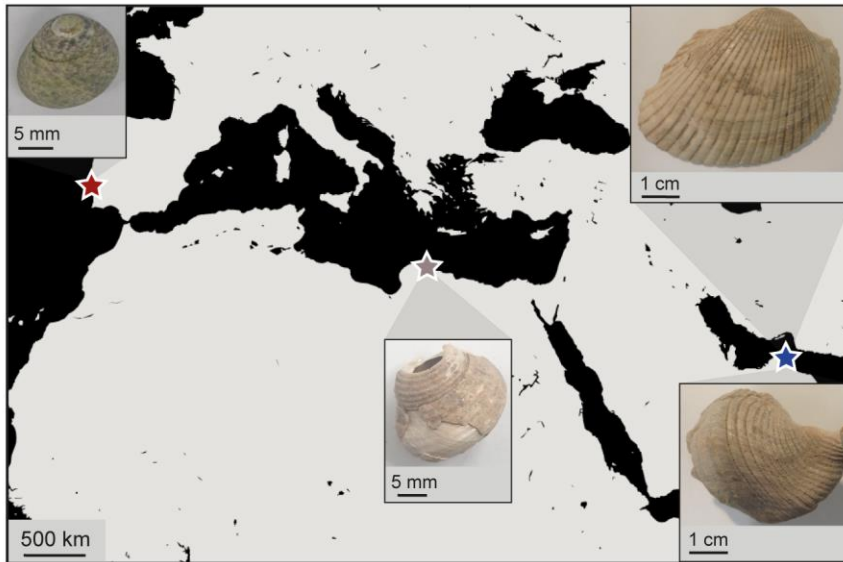
1019   245-249.

1020   Zolotoyabko, E., Pokroy, B., 2007. Biomineralization of calcium carbonate: structural aspects.

1021   CrystEngComm 9, 1156-1161. doi:10.1039/b710974a

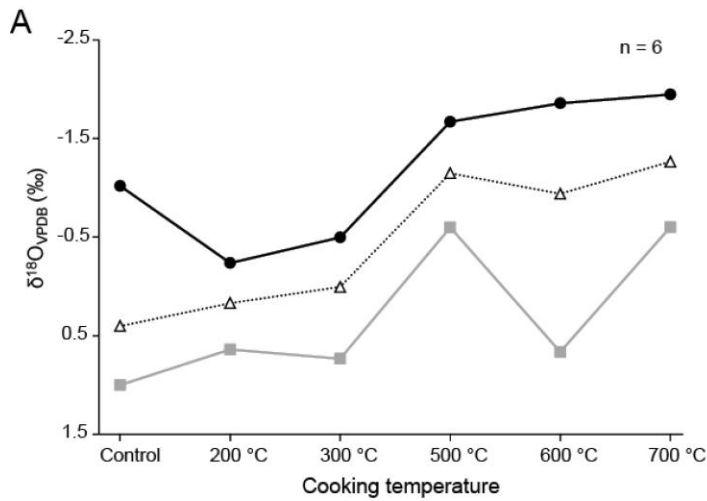1022

1023

1024

1025 Figure and tables

1026

1027 **Fig. 1.** Map showing the localities encompassed in the study. Red star: Praia do Tamariz, Portugal,

1028 where the modern *Phorcus lineatus* were collected. Grey star: Haua Fteah cave, Libya, where the

1029 archaeological *Phorcus turbinatus* were excavated. Blue star: sites in the UEA from which the

1030 archaeological remains of *Anadara uropigimelana* and *Terebralia palustris* were excavated.
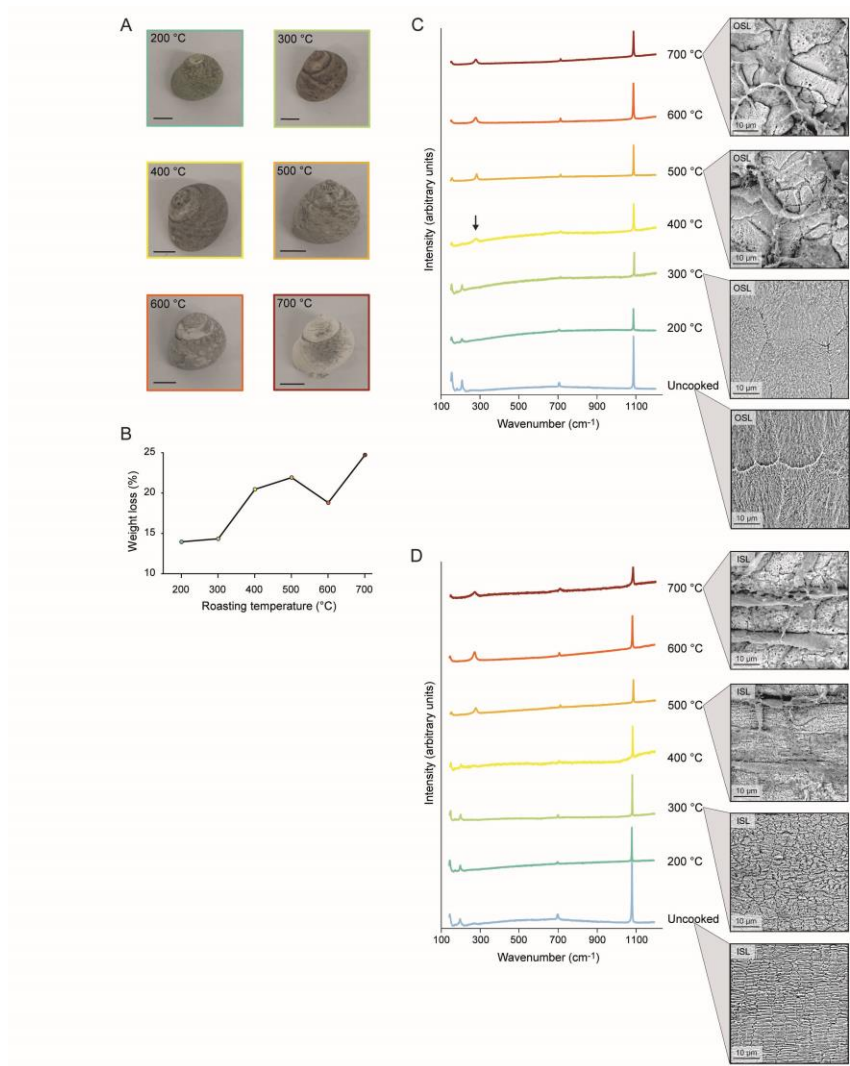
Fig. 2. Effects of the 5-minute heating experiment on *P. lineatus* shell. (A) Overall shell appearance after the thermal exposure at different temperatures. Scale bars = 5 mm. (B) Shell weight loss in response to heat. (C) Effect of heat on the outer shell layer (OSL) mineralogy and microstructures. The black arrow shows the extra peak in the 400 °C Raman spectrum indicating the transition phase from aragonite into calcite. (D) Thermal response of the inner shell layer (ISL) mineralogy and microstructures.

1031

1032

1033

1034

1035

1036

1037

A

δ¹⁸O_VPDB (‰)

n = 6

Control 200 °C 300 °C 500 °C 600 °C 700 °C

Cooking temperature

B

| Cooking temperature	δ¹⁸O_shell (p value)		
	5 min	20 min	60 min
100 °C	NA		
200 °C		NA	NA
300 °C			
500 °C			
600 °C		NA	NA
700 °C			

1038

1039 **Fig. 3.** Thermal behaviour of shell oxygen isotopes. (A) Oxygen isotope composition after roasting at
1040 the different temperatures. Gray squares=maximum $\delta^{18}O_{shell}$; open triangles=average $\delta^{18}O_{shell}$; black
1041 circles=minimum $\delta^{18}O_{shell}$. (B) The table refers to the different cooking durations tested in the present
1042 study and the previous study by Milano et al. (2016). Green cells indicate statistical similarity between
1043 isotope values of the heated and control shells ($p > 0.05$). Red cells indicate statistical difference ($p <$
1044 0.05). The yellow cell relates to a disagreement in the case of the specimen roasted at 300 °C for 20
1045 minutes. Its isotopic signature was statistically similar to the one of the control shell but different to the
1046 second control sample.

50
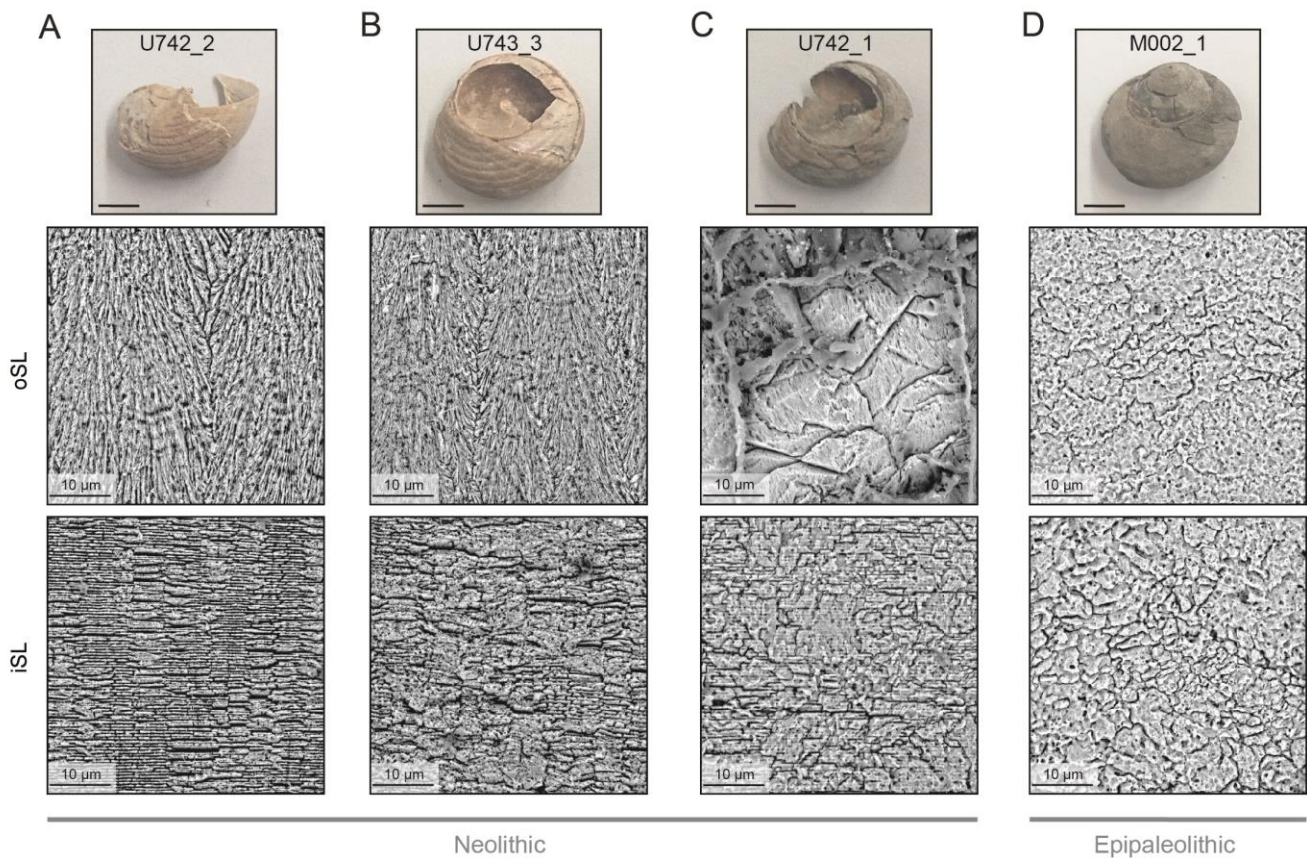
Fig. 4. Macroscopic appearance and microstructural organization of *P. turbinatus* shells from (A-C) Neolithic contexts and (D) Mesolithic contexts in the Haua Fteah cave. The first row of SEM images refers to the prismatic microstructures of the OSL. The second row displays the nacre platelets of the ISL. The visible changes in structural organization denote possible exposure to heating processes. Scale bars if not otherwise indicated = 5 mm.
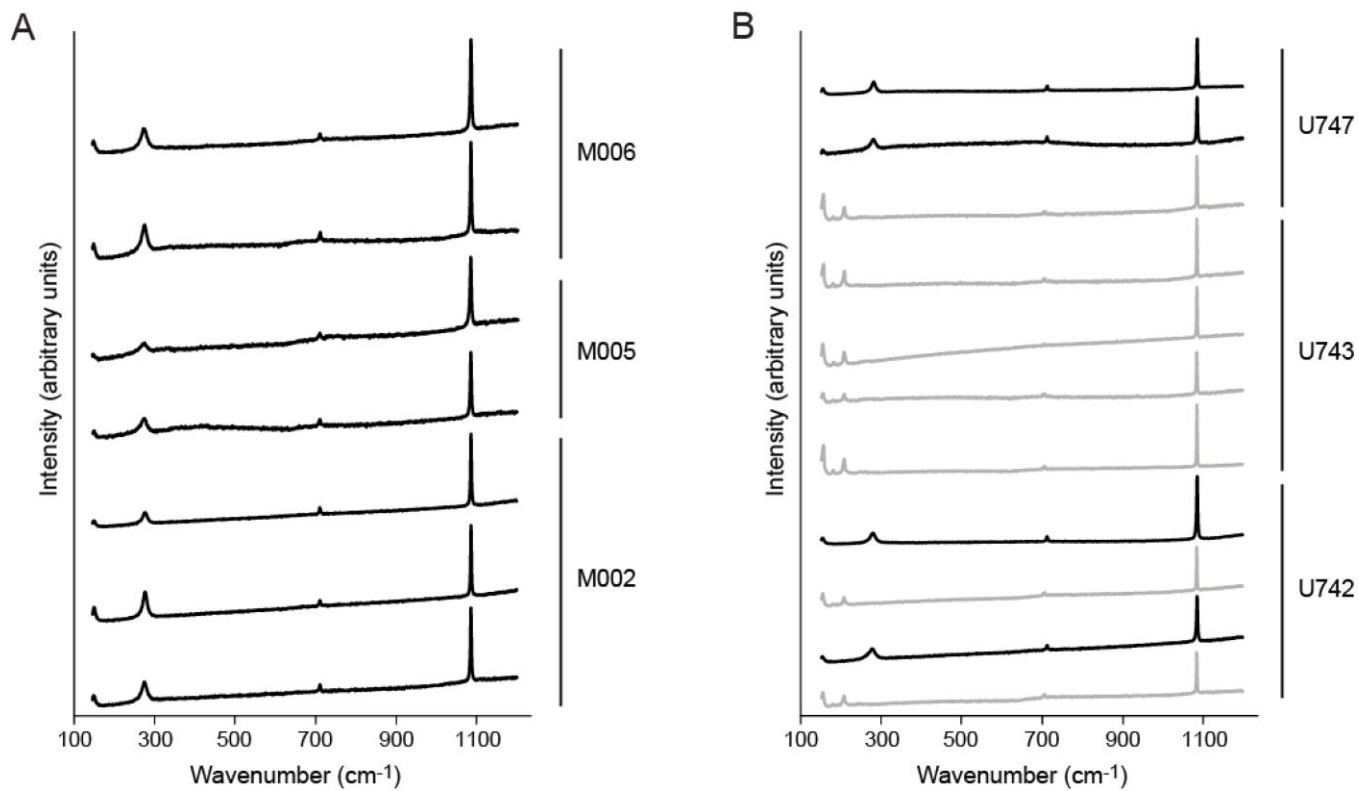
1053

Fig. 5. Raman spectra of *P. turbinatus* ISLs from (A) Neolithic contexts and (B) Mesolithic contexts in

the Haua Fteah cave. All Mesolithic specimens and four Neolithic specimens were calcitic (black lines);

the rest of the Neolithic specimens were aragonitic (grey lines).
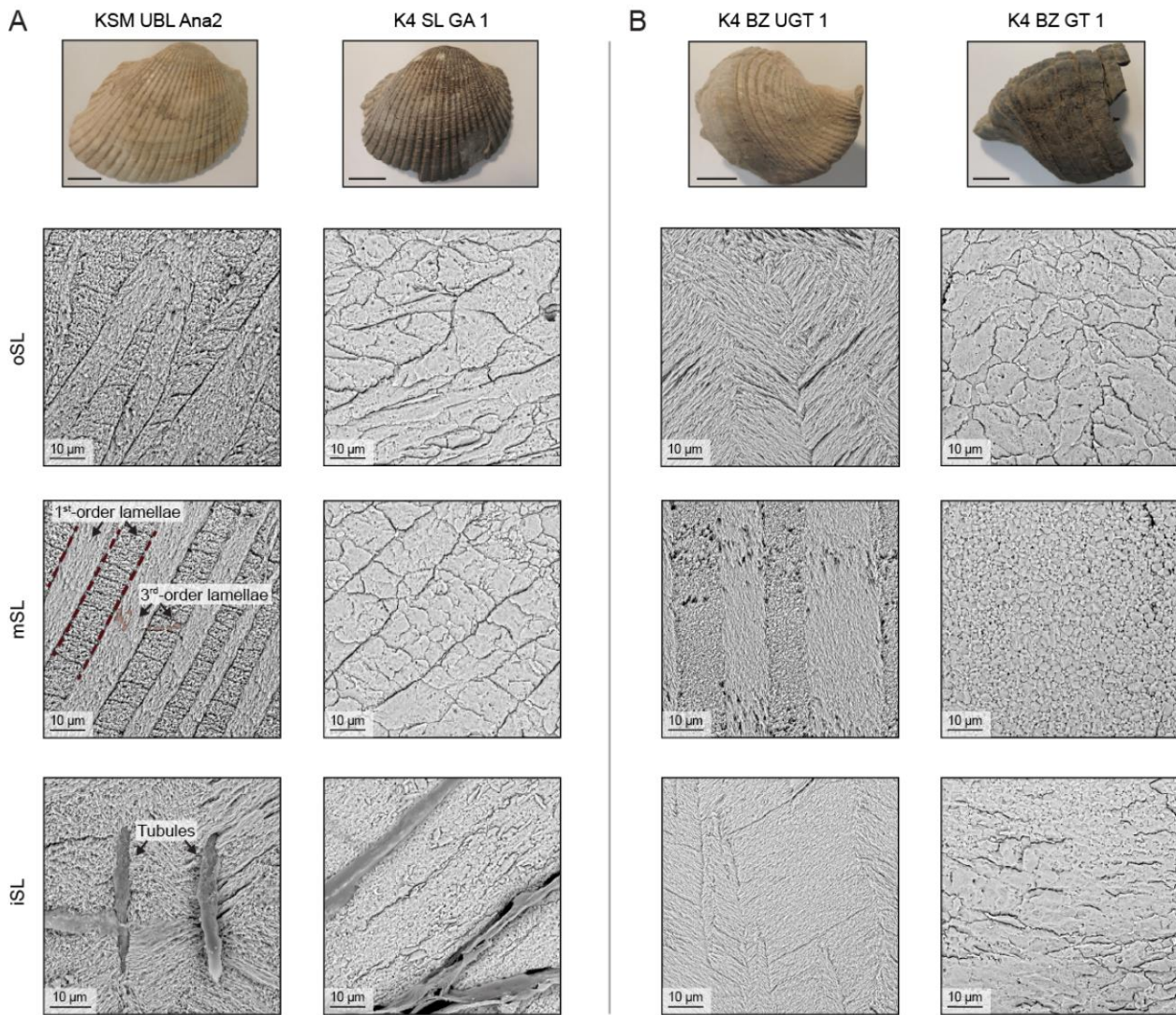
1057

Fig. 6. Macroscopic appearance and microstructural organization of the archaeological shells from the United Arab Emirates. (A) Whole shell and SEM images of two *A. uropigimelana* specimens. Shell KSM UBL Ana2 showed the typical microstructural architecture of the species. Highlights on the SEM images indicate the first and third order units of the crossed-lamellar structures as well as the organic microtubules perforating the shell material. Specimen K4 SL GA 1 shows the alteration of the overall color and microstructures, possible related to heat treatment. (B) Whole shell and SEM images of two *T. palustris* specimens with regular (K4 BZ UGT 1) and altered microstructures and appearance (K4 BZ UGT 1). Scale bars if not otherwise indicated = 1 cm.
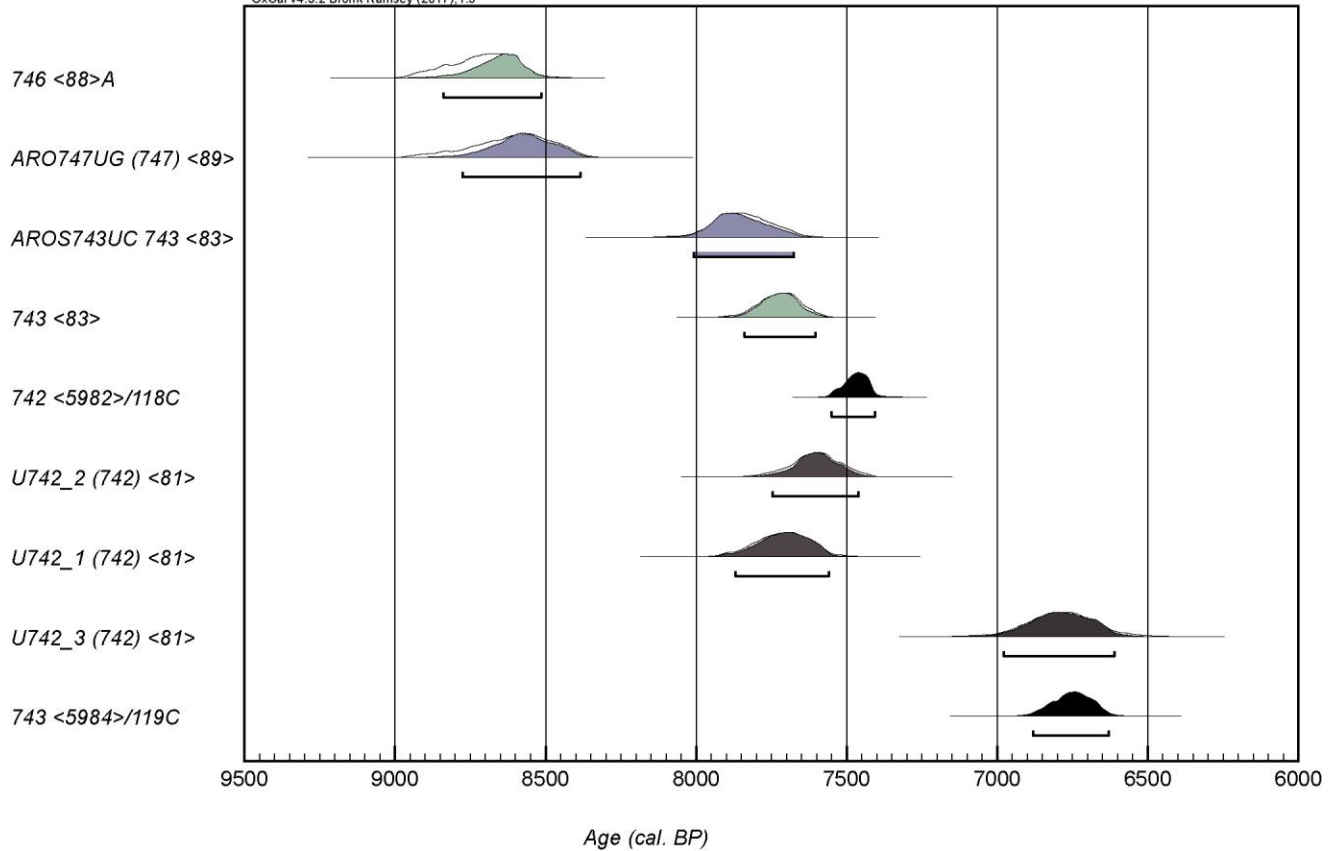
1066

1067   **Fig. 7.** Raman spectra of (A) *A. uropigimelana* and (B) *T. palustris* from the United Arab Emirates

1068   archaeological sites. Specimens K4 SL Ana2 and K4 BZ UGT 1 preserve their aragonitic OSL, MSL

1069   and ISL (grey lines). Specimens K4 SL GA 1 and K4 BZ GT 1 display calcite in all shell layers (black

1070   lines).
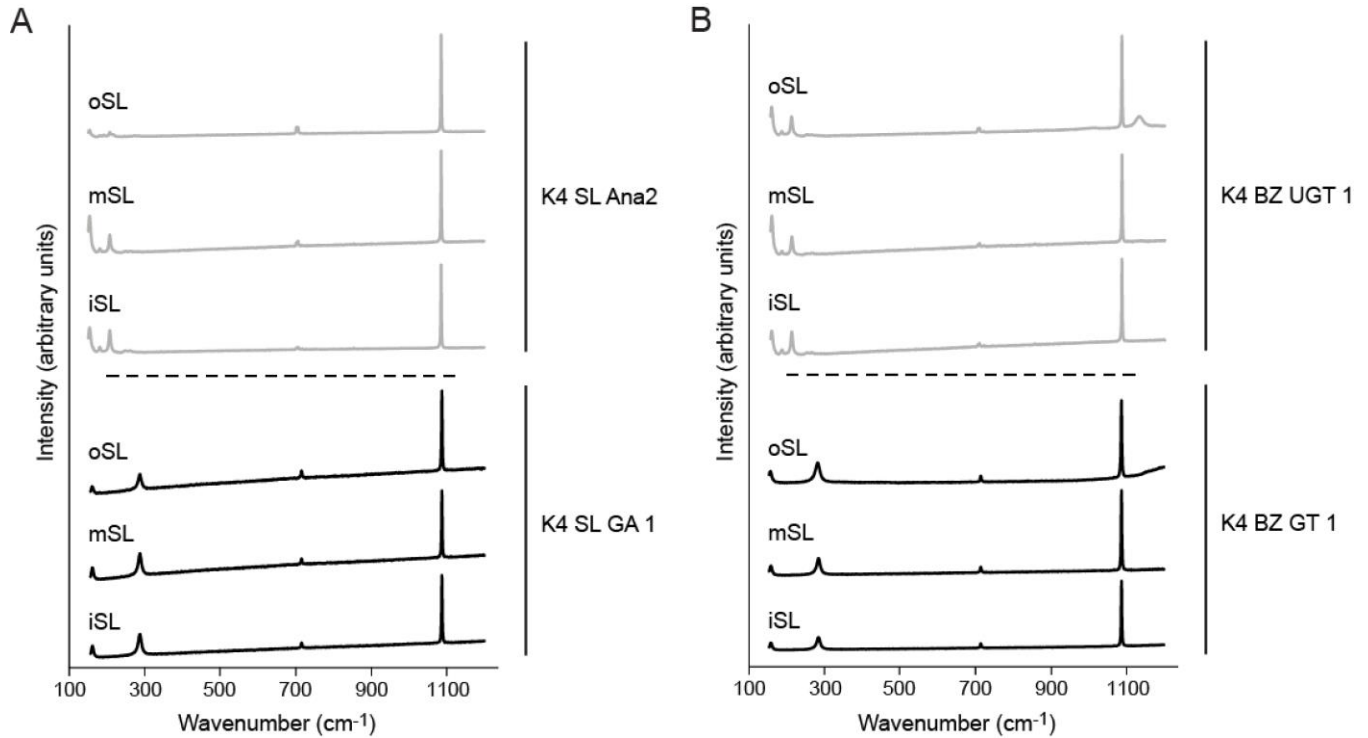
1071

1072   **Fig. 8.** Distribution of calibrated ^{14}C dates of Haua Fteah Trench U. Color-coding corresponds to the

1073   different materials used in the dating. Green = *H. Melanostoma* shells; blue = well-preserved *P.*

1074   *turbinatus*; grey = *P. turbinatus* from this study; black = charcoal.

1075

OxCal v4.3.2 Bronk Ramsey (2017); r:5

746 <88>A

ARO747UG (747) <89>

AROS743UC 743 <83>

743 <83>

742 <5982>/118C

U742_2 (742) <81>

U742_1 (742) <81>

U742_3 (742) <81>

743 <5984>/119C

9500 9000 8500 8000 7500 7000 6500 6000

Age (cal. BP)

1076

1077

1078 **Table 1.** List of studied specimens and details on their provenance.

ID	Species	Provenance	Period
A001	*P. lineatus*	Portugal	Modern
A001_M	*P. lineatus*	Portugal	Modern
A001_MR	*P. lineatus*	Portugal	Modern
A200	*P. lineatus*	Portugal	Modern
A200_M	*P. lineatus*	Portugal	Modern
A300	*P. lineatus*	Portugal	Modern
A300_M	*P. lineatus*	Portugal	Modern
A400	*P. lineatus*	Portugal	Modern
A400_M	*P. lineatus*	Portugal	Modern
A500	*P. lineatus*	Portugal	Modern
A500_M	*P. lineatus*	Portugal	Modern
A600	*P. lineatus*	Portugal	Modern
A600_M	*P. lineatus*	Portugal	Modern
A700	*P. lineatus*	Portugal	Modern
A700_M	*P. lineatus*	Portugal	Modern
M006_1	*P. turbinatus*	Haua Fteah, Libya	Capsian

M006_2	*P. turbinatus*	Haua Fteah, Libya	Capsian
M005_1	*P. turbinatus*	Haua Fteah, Libya	Capsian
M005_2	*P. turbinatus*	Haua Fteah, Libya	Capsian
M002_1	*P. turbinatus*	Haua Fteah, Libya	Capsian
M002_2	*P. turbinatus*	Haua Fteah, Libya	Capsian
M002_3	*P. turbinatus*	Haua Fteah, Libya	Capsian
U747_1	*P. turbinatus*	Haua Fteah, Libya	Neolithic
U747_2	*P. turbinatus*	Haua Fteah, Libya	Neolithic
U747_3	*P. turbinatus*	Haua Fteah, Libya	Neolithic
U743_1	*P. turbinatus*	Haua Fteah, Libya	Neolithic
U743_2	*P. turbinatus*	Haua Fteah, Libya	Neolithic
U743_3	*P. turbinatus*	Haua Fteah, Libya	Neolithic
U743_4	*P. turbinatus*	Haua Fteah, Libya	Neolithic
U742_1	*P. turbinatus*	Haua Fteah, Libya	Neolithic
U742_2	*P. turbinatus*	Haua Fteah, Libya	Neolithic
U742_3	*P. turbinatus*	Haua Fteah, Libya	Neolithic
U742_4	*P. turbinatus*	Haua Fteah, Libya	Neolithic
K4 SL Ana3	*A. uropigimelana*	Oman Sea	Bronze Age
K4 SL GA1	*A. uropigimelana*	Oman Sea	Bronze Age
K4 BZ GT1	*T. palustris*	Oman Sea	Bronze Age
K4 BZ UGT1	*T. palustris*	Oman Sea	Bronze Age
KSM UBL Ana2	*A. uropigimelana*	Oman Sea	Neolithic
KS Ana 1	*A. uropigimelana*	Oman Sea	Neolithic
KK1 Ana3	*A. uropigimelana*	Oman Sea	Neolithic

| KK1 Ana4 | *A. uropigimelana* | Oman Sea | Neolithic |

1082 **Table 2.** Reconstruction of shell exposure temperature by using shell overall appearance,
1083 microstructures and mineralogy as proxies in archeological specimens of *P. turbinatus*.

| Shell ID	Reconstructed cooking temperature		
	Macroscale appearance	Microstructures	Mineralogy
M006_1	600 °C	600 °C	≥ 500 °C
M006_2	600 °C	600 °C	≥ 500 °C
M005_1	600 °C	600 °C	≥ 500 °C
M005_2	600 °C	600 °C	≥ 500 °C
M002_1	600 °C	700 °C	≥ 500 °C
M002_2	600 °C	600 °C	≥ 500 °C
M002_3	600 °C	700 °C	≥ 500 °C
U747_1	500 °C	600 °C	≥ 500 °C
U747_2	500 °C	600 °C	≥ 500 °C
U747_3	500 °C	300 °C	< 500 °C
U743_1	300 °C	300 °C	< 500 °C
U743_2	300 °C	300 °C	< 500 °C
U743_3	300 °C	300 °C	< 500 °C
U743_4	300 °C	300 °C	< 500 °C
U742_1	400 °C	500 °C	≥ 500 °C
U742_2	Not cooked	Not cooked	< 500 °C
U742_3	500 °C	600 °C	≥ 500 °C
U742_4	500 °C	300 °C	< 500 °C

1084
1085

1086 **Table 3.** Trench U (Haua Fteah) ^{14}C dates. Symbol [*1] indicates dates corrected using reservoir offset of 58 ± 85
1087 ^{14}C years (Reimer and McCormac, 2002). Symbol [*2] indicates dates corrected using reservoir offset of 476 ± 48
1088 ^{14}C years (Hill et al., 2017).
1089

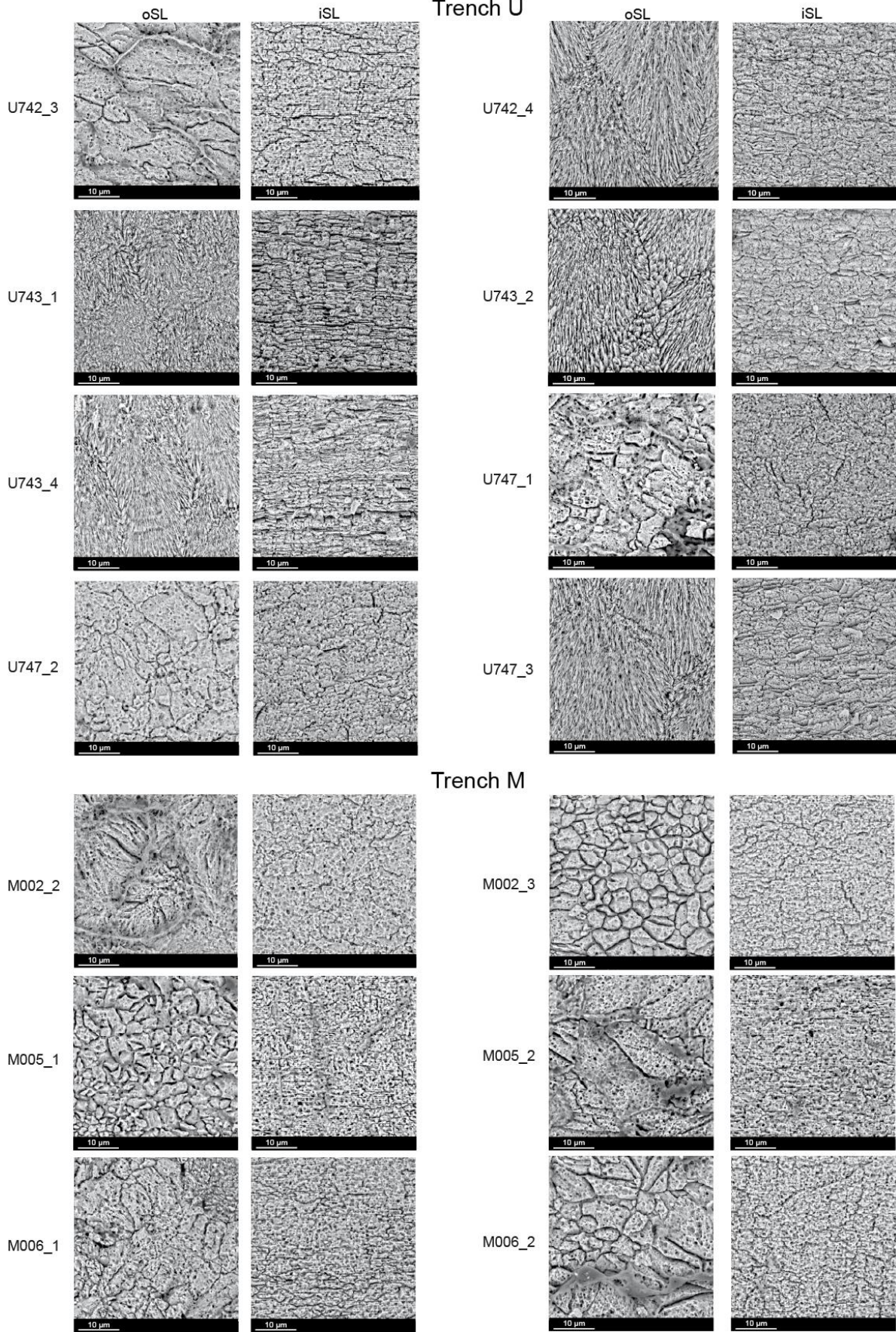| Sample ID	Lab Code	Material	Age (^{14}C yr)	±	Age (cal. BP) (unmodelled)	Age (cal. BP) (modelled)
U742_1	MAMS 30538 U742-1	*P. Turbinatus*	7300	21	7901 - 7556[*1]	7869 - 7560[*1]
U742_2	MAMS 30538 U742-2	*P. Turbinatus*	7184	21	7772 - 7438[*1]	7747 - 7461[*1]
U742_3	MAMS 30538 U742-3	*P. Turbinatus*	6378	21	7002 - 6558[*1]	6978 - 6610[*1]
ARO747UG	OxA-27391	*P. Turbinatus*	8171	37	8891 - 8381[*1]	8776 - 8385[*1]
ARO747UC	OxA-27490	*P. Turbinatus*	7447	35	8024 - 7652[*1]	8008 - 7675[*1]
742 <5982>/118C	UBA-28873	Charcoal	6965	39	7551 - 7405	7551 - 7405
743<5984>/119C	UBA-28874	Charcoal	6291	50	6883 - 6627	6880 - 6630
746 <88> A	UBA-25915	*H. Melanostoma*	8670	39	8930 - 8534[*2]	8840 - 8531[*2]
743 <83>	UBA-25912	*H. Melanostoma*	7732	37	7850 - 7590[*2]	7840 - 7605[*2]

1090

1091 Supplementary material
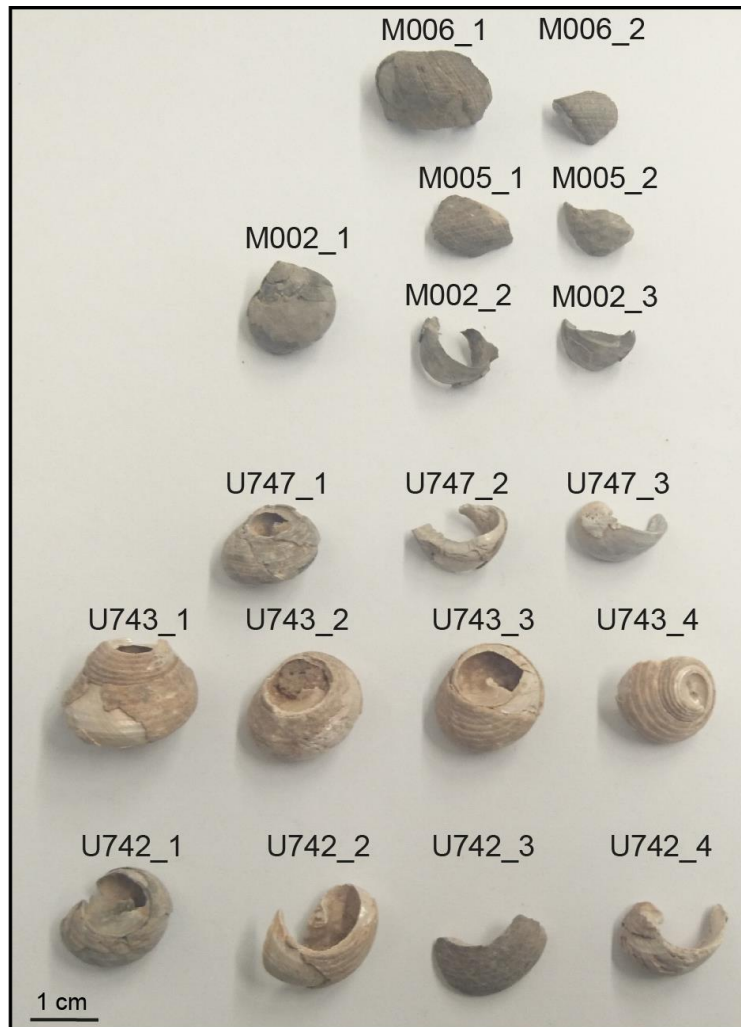
1094 **Fig. S1**. Overall appearance of all *P. turbinatus* excavated from Haua Fteah cave and used in the present study.

1095 The upper seven specimens were excavated from Trench M (Mesolithic). The rest of the specimens were

1096 excavated from Trench U (Neolithic).

1097

oSL	iSL	oSL	iSL

U742_3

U742_4

U743_1

U743_2

U743_4

U747_1

U747_2

U747_3

Trench M

M002_2

M002_3

M005_1

M005_2

M006_1

M006_2

1099

1100   **Fig. S2**.SEM images of the microstructural organization of *P. turbinatus* from Haua Fteah. Trench U = Neolithic

1101   context. Trench M = Mesolithic context.

1102
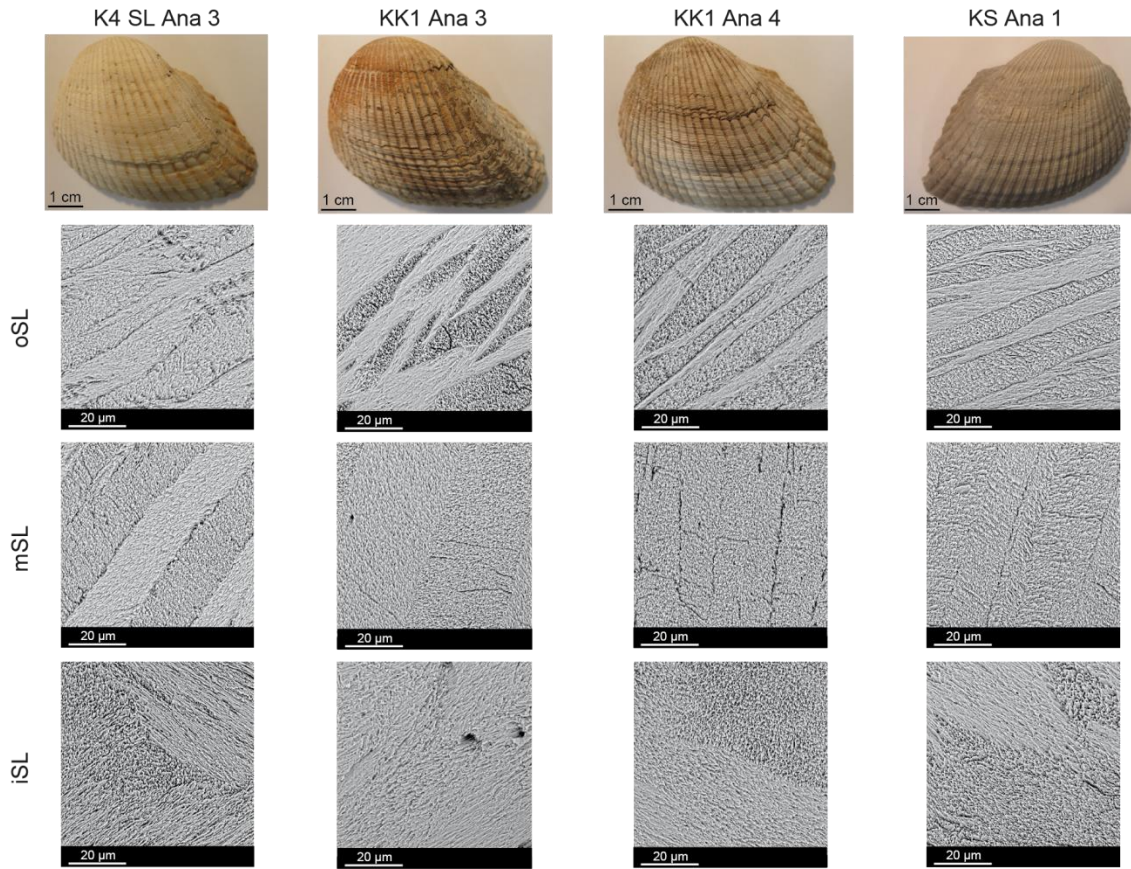
1103
1104
1105   **Fig. S3**. Overall appearance and microstructural organization of *A. uropigimelana* from Southeast Arabia.

1106
1107